Science
AAAS

Supplementary Materials for

Life-long persistence of nuclear RNAs in the mouse brain

Sara Zocher[1]†, Asako McCloskey[2,3]†, Anne Karasinsky[1], Roberta Schulte[2], Ulrike Friedrich[4,5,6], Mathias Lesche[4], Nicole Rund[1], Fred H. Gage[7], Martin W. Hetzer[8] *, Tomohisa Toda[1,9]*

*Corresponding authors: tomohisa.toda@fau.de; martin.hetzer@ist.ac.at

The PDF file includes:

Other Supplementary Materials for this manuscript include the following:

Materials and Methods

Experimental model

All procedures related to mouse care and treatment were approved by the Government of Saxony and the Institutional Animal Care and Use Committees of the Salk Institute for Biological Studies, and the experiments were performed in accordance with their guidelines.

For all experiments, C57BL/6 mice were group housed in standard cages under a 12 h light/dark cycle with *ad libitum* access to water and food. Both males and females were used in the experiments.

EU labelling and immunohistochemistry

5-Ethynyl-uridine (EU; Jena Bioscience, CLK-N002-10) was dissolved in PBS and injected subcutaneously into postnatal mice at 50 mg/kg/day. Animals were euthanized at the indicated time points by decapitation (postnatal mice) or cervical dislocation (adult mice). Pregnant dams received intraperitoneal EU injections at 100 mg/kg/day and embryos were collected after isoflurane anesthesia and decapitation of the mothers.

Collected brains were embedded in Tissue-Tek O.C.T. Compound (Science Services) and fresh frozen using dry ice. Brains were sliced into 14 µm sections using a cryostat (Leica). Sections were fixed with 4% paraformaldehyde (PFA; Sigma-Aldrich) in PBS for 10 min at room temperature (RT), washed with PBS and permeabilized with 0.5% Triton X-100 (Carl-Roth) in PBS for 30 min at RT. EU was visualized using Click-iT™ Plus Alexa Fluor™ 555 Picolyl Azide Toolkit (Life Technologies, C10642) with incubation of Alexa Fluor 555 PCA on brain sections for 30 min at RT. For the combination of EU click chemistry with immunohistochemistry, EU signals were fixed with 4% PFA for 5 min at RT. Subsequently, sections were washed with PBS and unspecific binding was blocked for 1 h in blocking solution (10% donkey serum, 0.2% Triton X-100 in PBS). Primary antibodies were incubated overnight at 4°C as follows: rat anti-Sox2 (eBioscience, RRID:AB_11219471), mouse anti-NeuN (EMD Millipore, MAB377) or rabbit anti-NeuN (Abcam, ab104225, RRID:AB_10711153), rabbit anti-GFAP (Abcam, ab7260, RRID:AB_305808), rabbit anti-NeuroD1 (Abcam, ab213725, RRID:AB_2801303), rat anti-Ki67 (eBioscience, #14-5698-82, AB_10854564). The following secondary antibodies were applied; donkey anti-rat IgG Alexa 488 (Sox2, Ki67; Jackson ImmunoResearch, #712-545-153) or donkey anti-mouse IgG Alexa 647 (NeuN; Jackson ImmunoResearch, #715-605-151) and donkey anti-rabbit IgG Alexa 647 (NeuN, GFAP, Neuro D1; Jackson ImmunoResearch, #715-605-152). Secondary antibodies were incubated together with Hoechst or DAPI (1:10,000; Jackson ImmunoResearch) for 2 h at RT. All antibodies were diluted in 3% donkey serum and 0.2% Triton X-100 in PBS. Slides were washed in PBS and mounted with Prolong Gold anti-fade reagent (Invitrogen, P36930).

BrU labelling and immunohistochemistry

5-Bromouridine (BrU; Sigma-Aldrich, #850187) and 5-Bromouridine 5-triphosphate (BrUTP; Sigma-Aldrich, B7166) were dissolved in PBS and injected subcutaneously into postnatal mice at 50 mg/kg/day. Brains were collected and processed as described for EU labelling. For detection of BrU and BrUTP in tissue, antigen retrieval was performed. Briefly, sections were incubated in pre-heated 2 M hydrogen chloride for 20 min at 37°C. Following multiple washing steps in PBS, immunohistochemistry was performed as described above. BrU and BrUTP were detected using rat anti-BrdU antibody (clone BU1/75 ICR1; Novus Biologicals, NB500-169) combined with secondary Cy3 donkey anti-rat IgG (Jackson ImmunoResearch, #712-165-153).

RNase and DNase I treatments

Brain sections were fixed and permeabilized and treated with either 10 U Shortcut RNase III (0.2 U/µl; NEB, M0245S) and 5 µg RNase A (1 mg/ml; Thermo Fisher Scientific, EN0531) or diluent alone for 2 h at 37°C. For DNA digest, sections were treated with 0.125 U/µl DNase I (NEBm M0303S) or 5 U RQ1 RNase-free DNase (0.1 U/µl; Promega, M6101) at RT for 20 h. Slides were washed in PBS and click reaction was performed using the Click-iT™ Plus Alexa Fluor™ 555 Picolyl Azide Toolkit as described above. EdU (5-Ethynyl-2-deoxyuridine, Thermo Fisher Scientific) was detected using the same protocol as applied for EU. DNA was stained with Hoechst dye or DAPI (1:4,000) in PBS for 10 min at RT.

For RNase and DNase I treatments on cells, NPCs were fixed with 4 % PFA in PBS, washed with PBS, permeabilized with 0.5 % Triton X-100 in PBS, and incubated in the presence of 1 mg/ml of RNase A (Thermo Fisher Scientific, EN0531) or 10 U of RNase H (NEB, M0297S) or 4 U of TURBO DNase (Thermo Fisher Scientific, AM2238) for 1 h at 37°C, followed by EU-Click-iT reaction and staining of nuclei with DAPI (1:4000, 10 min).

Cell culture and drug treatments

Mouse (C57BL/6) NPCs were isolated and cultured as described previously (*25*) with minor modifications. NPCs were cultured in DMEM/F-12 medium (Thermo Fisher Scientific, #11330057) supplemented with N2 (Life Technologies, #7502001) and B27 (minus vitamin A; Life Technologies, #12587001), laminin (0.5 µg/ml; Sigma-Aldrich, #11243217001) in the presence of FGF2 (10 ng/ml; PeproTech, 100-18C), EGF (10 ng/ml; PeproTech, AF-100-15), and heparin (5 µg/ml; Sigma-Aldrich, H3149). For the induction of quiescence, NPCs were plated with FGF2 (20 ng/ml) and BMP4 (20 ng/ml; R&D Systems, 314-BP-050/CF) and cultured for the indicated number of days. EU was added to the medium at a final concentration of 250 µM. BrU was added at a final concentration of 1 mM. To analyze cell proliferation, BrdU was added to the culture medium for 4 h at a final concentration of 10 µM.

For RNA polymerase inhibition during EU treatment, RNA polymerase inhibitors ML60218 (40 µM; MedChemExpress, HY-122122) and α−Amanitin (1 ng/µl; AppliChem, A1485) were applied 1 day after induction of quiescence for a period of 4 h. EU was added at 2 h after application of RNA polymerase inhibitors and washed out by medium change after a 2 h incubation period. For RNA polymerase inhibition following EU treatment, NPCs were labelled with EU one day after induction of quiescence for 24 h. EU was then washed out and NPCs were incubated with ML60218 (20 µM) or α−Amanitin (1 ng/µl) for 24 h before they were analyzed.

For inhibition of ribonucleotide reductases, NPCs were treated with hydroxy urea (0.3 mM; Sigma-Aldrich, H8627) or thymidine (6 mM; Sigma-Aldrich, T1895). The efficacy of the inhibitors was confirmed by measuring the incorporation of EdU in proliferating NPCs. The inhibitors were applied with EU in quiescent NPCs (quiNPCs), and the incorporation of EU was analyzed 24 h after the treatment.

Manipulation of *satRNAs* in NPCs

Locked nucleic acid (LNA)-DNA-GapmeRs (Qiagen/Exiqon) were previously described (*18*) and delivered to NPCs by nucleofection (Mouse Neural Stem Cell Nucleofector Kit, Lonza). Briefly, NPCs were suspended in 100 µl nucleofector solution (Lonza) and then mixed with LNA-DNA GapmeRs (500 nM in final concentration). Transfection was conducted in an electroporation cuvette using a nucleofector instrument (Lonza). Transfected cells were plated in fresh medium to induce quiescence and incubated for 24 h before medium was replaced. Afterwards, the medium

was changed every 48 h. For the reactivation of quiNPCs, cells were detached with Accutase (Sigma-Aldrich, A6964) and re-plated in proliferation medium containing FGF2 and EGF (both 20 ng/ml).
SgRNAs for CRISPR-based manipulation of *minor* and *major satRNAs* were previously described (*19*). SgRNAs were cloned into pU6-sgRNA/EF1a-mCherry (Addgene plasmid #114199; gift from Jeremy Day). For CRISPRa, we cloned a puromycin resistance gene into CAG-FLAG-dCas9-VPR (Addgene plasmid #114197; gift from Jeremy Day) using AvrII and FseI restriction sites (replacing bleomycin). Puromycin was amplified from pX459 V2.0 (Addgene plasmid #62988; gift from Feng Zhang). Proliferating NPCs were co-transfected (nucleofection) with pU6-sgRNA/EF1a-mCherry and CAG-FLAG-dCas9-VPR-Puromycin (CRISPRa) or SFFV-KRAB-dCas9-P2A-mCherry (Addgene plasmid #60954; gift from Jonathan Weissman; CRISPRi). Transfected cells were selected using puromycin (1 µg/ml; Thermo Fisher Scientific, A1113803) for 48 h (CRISPRa) or using fluorescence activated cell sorting (FACS) for mCherry (CRISPRi) and re-plated in proliferating or quiescence conditions as indicated in the figure legends.

Perturbation of heterochromatin in NPCs
Histone methyltransferase inhibitors Chaetocin (2.5 nM or 5 nM; Cayman Chemical, Cay13156-500) and Bix01294 (250 nM; Cayman Chemical, Cay13124-1) were dissolved in DMSO and applied upon induction of quiescence or to already quiNPCs as indicated. Control NPCs were treated with an equal volume of DMSO. *Cbx1* knock-out NPC lines were generated as previously described (*26*). Briefly, we used 2 sgRNAs to delete a 760-bp fragment targeting the first coding exon and confirmed the deletion using PCR with gene-specific primers and Sanger sequencing. SgRNAs and primers are listed in Table S1.

Immunocytochemistry
Immunocytochemistry was performed as previously described (*25*), with slight modifications. Briefly, NPCs were fixed with 4% PFA for 10 min at RT followed by 3 washes with PBS and then permeabilized with 0.1% Triton X-100 in TBS, blocked with 3% horse serum and incubated with primary antibodies for 2 h with mouse anti-Ki67 (BD Pharmingen, B56), anti-BrdU (clone BU1/75 ICR1; Novus Biologicals, NB500-169), rabbit anti-H3K9Me3 (Abcam, ab8898, RRID:AB_306848). For BrdU staining, cells were incubated with 2 M HCl for 10 min at 37°C before blocking. For BrU stainings, cells were incubated in PBS with 0.2 % Triton X-100 at 70 °C for 10 min before blocking. BrU was visualized using rat anti-BrdU antibody (clone BU1/75 ICR1; Novus Biologicals; 1:250).

Imaging and image analyses
Fluorescence was detected using a Zeiss LSM 980 or SP8 Leica confocal microscope. Images were acquired with 20x, 40x or 63x objectives with z-stack series. The density and cell types of EU^+ cells were measured using the cell counting function in Fiji. The area of regions of interests were measured using DAPI/Hoechst signals. The fractions of co-labelled EU^+ cells in the DG, CB and S1 were counted from 3-4 animals at each time point except for 2-year-old animals (n = 2). For *in vitro* analyses, z-stack images were taken from at least 3 randomly selected slide positions and the total intensity of H3K9Me3 and EU signals was measured for all nuclei in the field of view.

qRT-PCR for EU-labeled transcripts

Frozen tissue was homogenized on ice in Trizol (Ambion) for 30 s with a pellet pestle motor (Contes). After 4 min on ice, RNA was extracted and purified using the miRNeasy Mini Kit (QIAGEN), including DNase I in-column digestion. In total, RNA samples were treated with DNase three times to avoid contamination with genomic DNA. Purified RNAs were treated with RQ1 DNase (Promega, M6101), re-purified and then EU-labeled transcripts were enriched using Click-iT Nascent RNA Capture Kit (Thermo Fisher Scientific, C10365). Reverse transcription was performed on T1 Streptavidin beads with SuperScript IV VILO Master Mix with ezDNase treatment (Thermo Fisher Scientfic, #11766050). Quantitative PCR was performed using SYBR Green PCR Master Mix (Thermo Fisher Scientific, #4364344) with serially diluted cDNA synthesized from input and pulldown RNAs. Enrichment of EU-labeled transcripts was measured by comparing the fraction of pulled-down transcripts between EU-treated samples and PBS-treated samples. Sequences of primers are listed in Table S1.

BRIC-qPCR

RNA was isolated using Trizol (Ambion) and treated with RQ1 DNase (Promega, M6101). After re-purification of RNA, BRIC-qPCR was performed as previously described (*27*). Briefly, mouse anti-BrdU antibody (MBL, 2B1) was incubated with Protein G Dynabeads (Thermo Fisher Scientific), and washed with ice-cold BSA/Triton X-100/PBS solution. RNA from PBS-treated and BrU-treated NPCs was incubated with beads for 2 h, and beads were washed. cDNA synthesis and qPCR were performed as described for EU-labeled transcripts. PBS-treated samples were used as a control.

Statistics

Statistical analyses were performed using R, Prism 9 and Excel (Microsoft). P-values were determined by an unpaired Student's *t*-test, a Welch's *t*-test, a one-sample *t*-test, a Mann-Whitney U test, Kruskal-Wallis test, or paired ratio *t*-test. Sample sizes were determined based on previous experience with animal and cell culture models. At least 3 experiments were conducted (unless otherwise specified in the figure legends), and values from individual cells, animals or experiments were plotted. Replicates in animal experiments represent individual mice. No animals were excluded from the analysis. The same mice injected with EU at P3-5 and analyzed at P6 (24 h chase period; referred to as 1-week-old mice) were used for the analysis of EU signal distributions in Figures S2-3, S7, S10C and for the comparison of EU signal intensities with 1-year-old mice (Fig. S4). For cell cultures, replicates correspond to independent experiments with the same NPC line.

Further statistical details are reported in the figure legends.

EU-RNA-Sequencing and analysis

EU-RNA-Sequencing was performed as previously described (*28*) with minor modifications. For quiNPCs, sequencing was performed on EU-labeled and non-EU-labeled (PBS-treated) quiNPCs from 3 experiments. For hippocampus tissue, sequencing was performed on 3 mice that were injected with EU and 3 mice that were injected with PBS (vehicle). RNA was isolated using Trizol (Ambion; NPCs) or miRNeasy Micro Kit (QIAGEN; hippocampal tissue) and genomic DNA was digested with RQ1 DNase (Promega, M6101). RNA was re-purified using miRNeasy Micro Kit (QIAGEN) with gDNA removal columns. EU-labeled transcripts were enriched using Click-iT Nascent RNA Capture Kit (Thermo Fisher Scientific, C10365) and the same enrichment protocol was applied to RNA from non-EU(PBS)-labeled samples. To assess pull-down

efficiencies, we used previously described biotinylated spike-in sequences (*28*). Sequencing libraries were prepared using Universal Plus Total RNA-Seq library preparation Kit (TECAN) with RNA fragmentation and cDNA synthesis performed on Streptavidin-coated beads (T1 Dynabeads, Thermo Fisher Scientific). Library quality was confirmed using Bioanalyzer (Agilent) and libraries were sequenced on NovaSeq 6000 (Illumina) to reach 80 Mio paired-end reads. Libraries were demultiplexed using bcl2fastq2 (v2.20.0) and unique molecular identifier information was extracted using UMI-tools (v1.1.2). Reads were mapped to the mouse reference genome GRCm39 using Ensembl gene annotation version 104 and STAR (v2.7.10b). Aligned fragments were deduplicated based on unique molecular identifiers and mapping coordinates using UMI-tools (v1.1.2). Fragments per gene and sample were summarized using *featureCounts* (v2.0.1) (*29*). EU-enriched RNAs were defined as transcripts that were significantly enriched in EU-treated samples compared to PBS-treated samples as determined using edgeR (*30*) (adjusted $p < 0.05$ (Benjamini-Hochberg) and fold change > 2). Pie charts depicting gene class distributions refer to percentages of RNA types among significantly EU-enriched gene-derived RNAs. Enrichment of RNA types in EU-pulldown samples was assessed by binomial regression using the function *glm* in R. Odds ratios are the exponential coefficients of the model. Pathway analysis was performed using ReactomePA (*31*) with EU-enriched genes as query list and all quiNPC-expressed genes as background list. To facilitate visualization of EU-enriched genes in quiNPCs in the MA plot, genes with $-\log_{10}$(adjusted *p*-value > 10) were not plotted (a total of 4 genes). For analysis of repetitive RNAs, repetitive sequences were retrieved from *RepeatMasker* (*32*) and sequencing reads were aligned using *kallisto*. EU-enriched repeat RNAs were identified using *Sleuth* (*33*) applying Wald test to detect significant enrichment in EU-treated samples compared to PBS-treated samples with Benjamini Hochberg-adjusted *p*-value thresholds (*q*-value) of 0.05. Pie charts depicting repetitive element type composition refer to percentages of each repeat RNA type (transcript per million per repeat type) within EU-enriched repetitive RNAs.

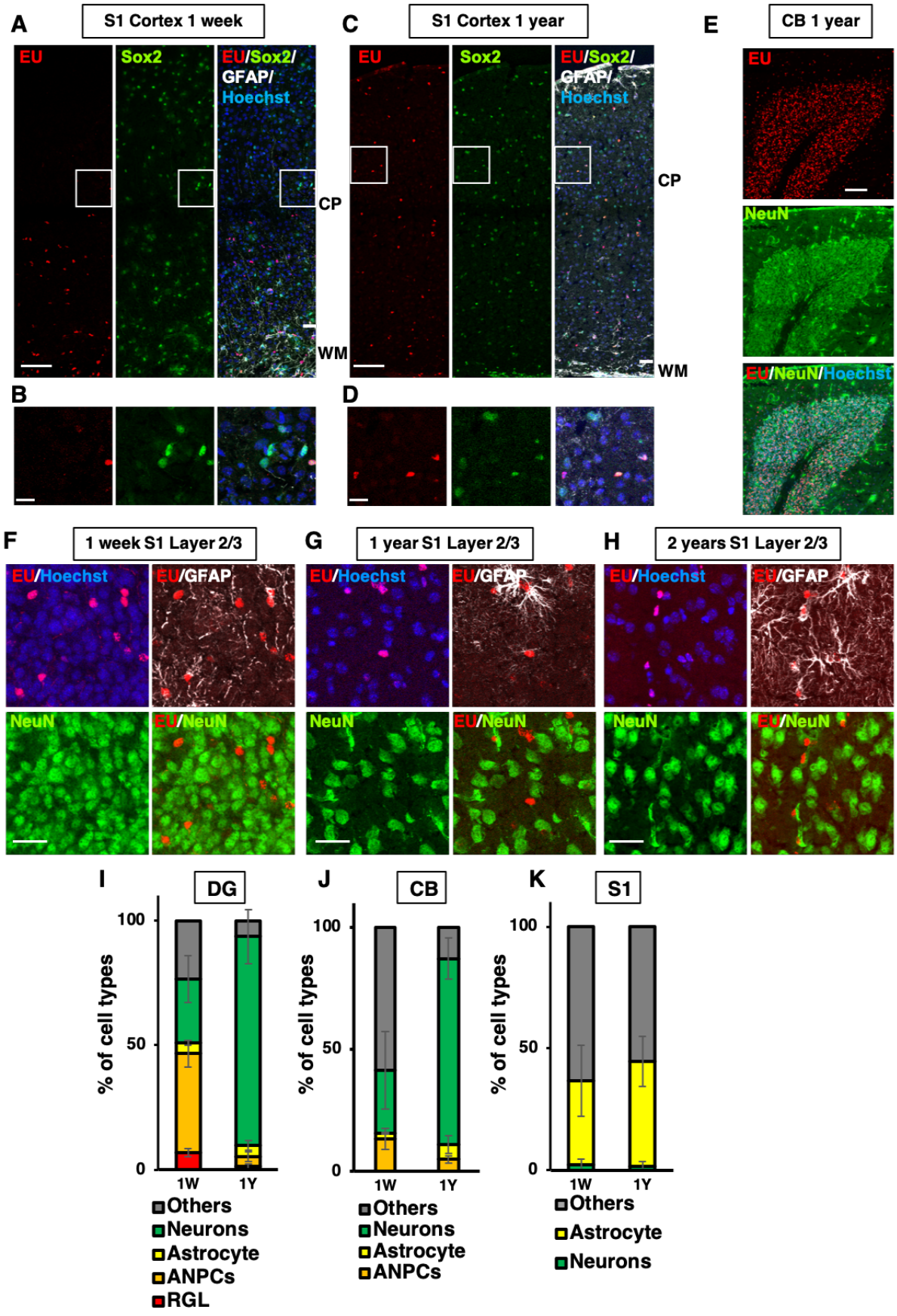
A
S1 Cortex 1 week
EU
Sox2
EU/Sox2/
GFAP/
Hoechst
CP
WM
B
C
S1 Cortex 1 year
D
E
CB 1 year
NeuN
EU/NeuN/Hoechst
F
1 week S1 Layer 2/3
EU/Hoechst
EU/GFAP
NeuN
EU/NeuN
G
1 year S1 Layer 2/3
H
2 years S1 Layer 2/3
I
DG
J
CB
K
S1
% of cell types
100
50
0
1W
1Y
Others
Neurons
Astrocyte
ANPCs
RGL

Fig. S1.

Distribution of EU$^+$ cells in the mouse brain. Mice were injected with EU at P3-P5 and analyzed at P6 (1 week) or at an age of 1 or 2 years. (**A-B**) Sparse distribution of EU$^+$ cells in the primary somatosensory (S1) cortex of 1-week-old and 1-year-old animals. (**C-D**) High magnification images from the insets of A and B. Some EU$^+$ cells colocalized with Sox2$^+$ cells. (**E**) Distribution of EU$^+$ cells in the cerebellum (CB) of a 1-year-old animal. (**F-H**) Retention of EU signals in GFAP$^+$ cells in S1 in 1-week-old, 1-year-old and 2-years-old mice. (**I-K**) Fractions of cell types among EU$^+$ cells in the DG, CB and S1. The composition of EU$^+$ cells in the DG, CB and S1 was measured from 1-week-old (1W) and 1-year-old (1Y) animals (n = 3-4 mice). Neurons, NeuN$^+$ cells. ANPCs, adult neural progenitor cells, Sox2$^+$ cells. RGL, radial glia-like adult neural stem cells, Sox2$^+$ with a GFAP$^+$ radial fiber. Astrocyte, GFAP$^+$ cells. Scale bars, 100 μm (A, C, E), 20 μm (B, D, F, G, H).

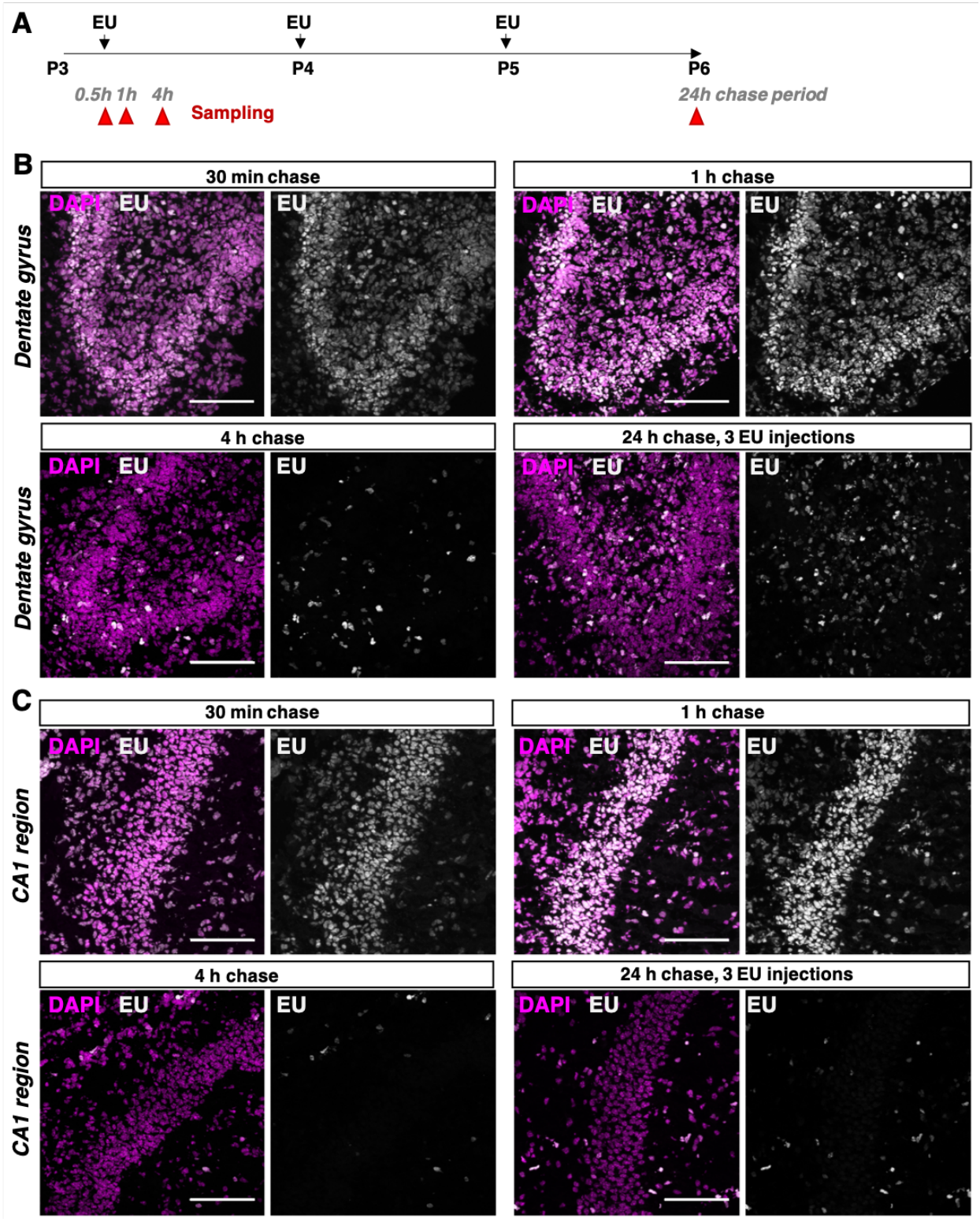

Fig. S2.

Spatiotemporal dynamics of EU-labelled cells in the hippocampus after EU injection. (**A**) Mice were injected with EU at P3 and analyzed 30 min, 1 h or 4 h after EU injection. Another

cohort of mice received daily EU injections at P3-P5 and was analyzed at P6 (24 h after the last EU injection) – those mice were identical to the 1-week samples analyzed in fig. S4 (to be able to compare EU signals, sample collections at 0.5 h to 1 year after EU injection were performed in one continuous experiment). Shown are EU stainings of the hippocampal dentate gyrus (**B**) and CA1 region (**C**). Scale bars, 100 μm.

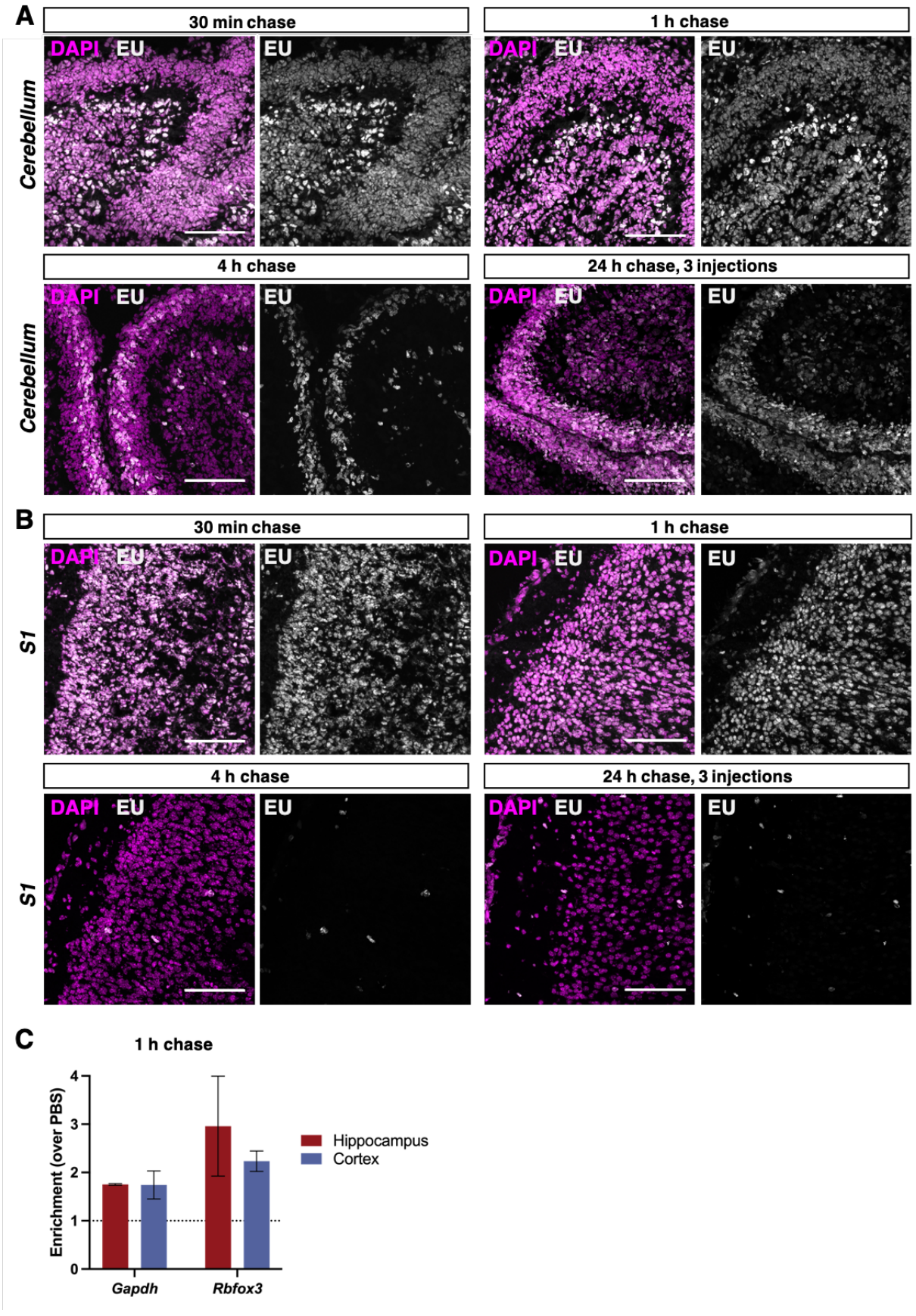
A
30 min chase
1 h chase
DAPI EU
EU
Cerebellum
4 h chase
24 h chase, 3 injections
B
S1
C
1 h chase
Enrichment (over PBS)
0
1
2
3
4
Hippocampus
Cortex
Gapdh
Rbfox3

Fig. S3.

Spatiotemporal dynamics of EU-labelled cells in the cerebellum and cortex after EU injection. Injection scheme identical to Fig. S2A. While high numbers of EU label-retaining cells were observed at 24 h after EU injection in the cerebellum (**A**), only very few EU label-retaining cells were observed in cortical areas (**B**). Scale bars, 100 μm. (**C**) Pulldown of EU-labelled transcripts at 1 h after EU injection confirms RNA labelling by EU in hippocampus and cortex. Shown is fold enrichment as determined by qPCR with mean ± SEM from 2 EU injected mice compared to 2 PBS injected mice.

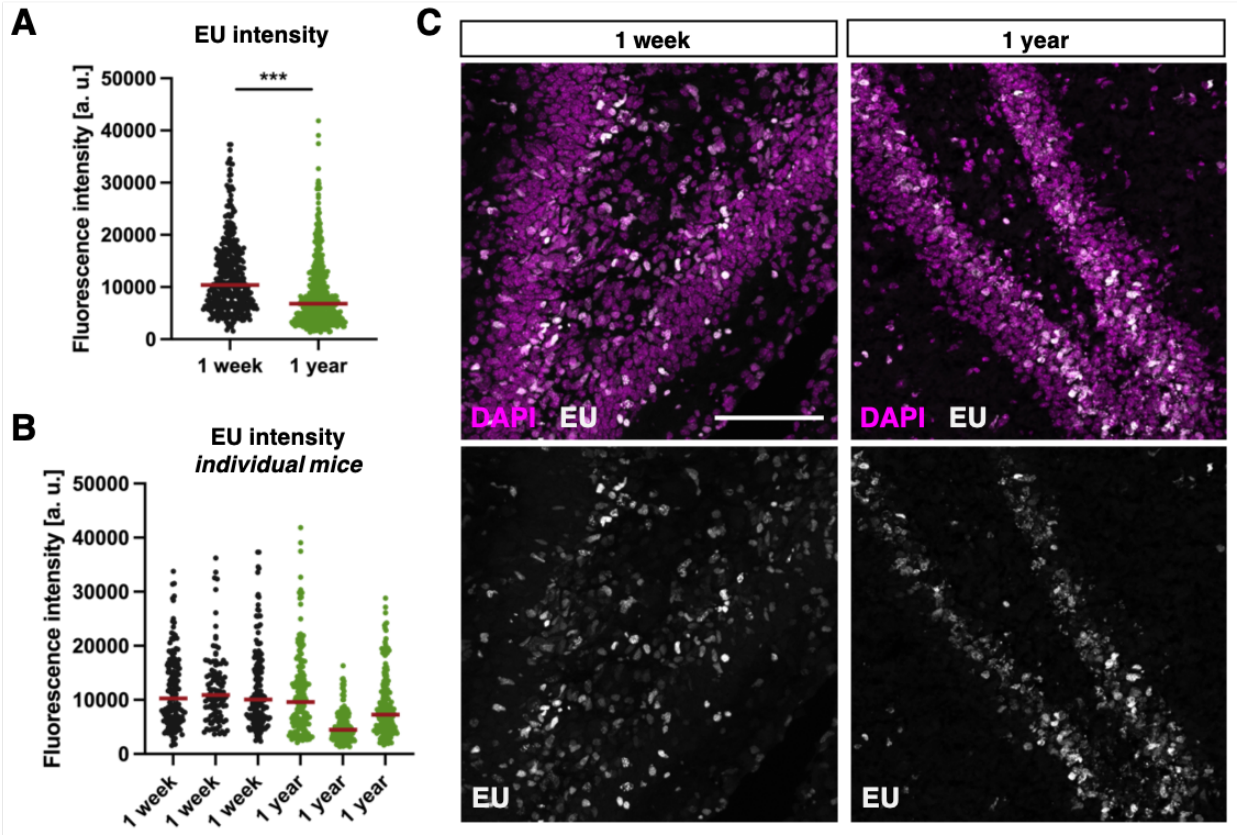

Fig. S4.

Comparison of EU signal intensities between 1-week-old and 1-year-old mice. All mice were injected with EU at P3-P5 and analyzed at P6 (1-week-old mice) or 1 year later (1-year-old-mice). (**A**) Quantification of nuclear EU signal intensities in the dentate gyrus. Depicted are individual nuclei with group medians (***$P < 0.001$, Wilcoxon-Mann-Whitney test, n = 3 animals per age). Cells were quantified on multiple sections per animal. (**B**) Nuclear EU signal intensities split by individual animal. (**C**) Representative fluorescent images of EU signals in the dentate gyrus of 1-week-old mice and 1-year-old mice. Scale bar, 100 µm.

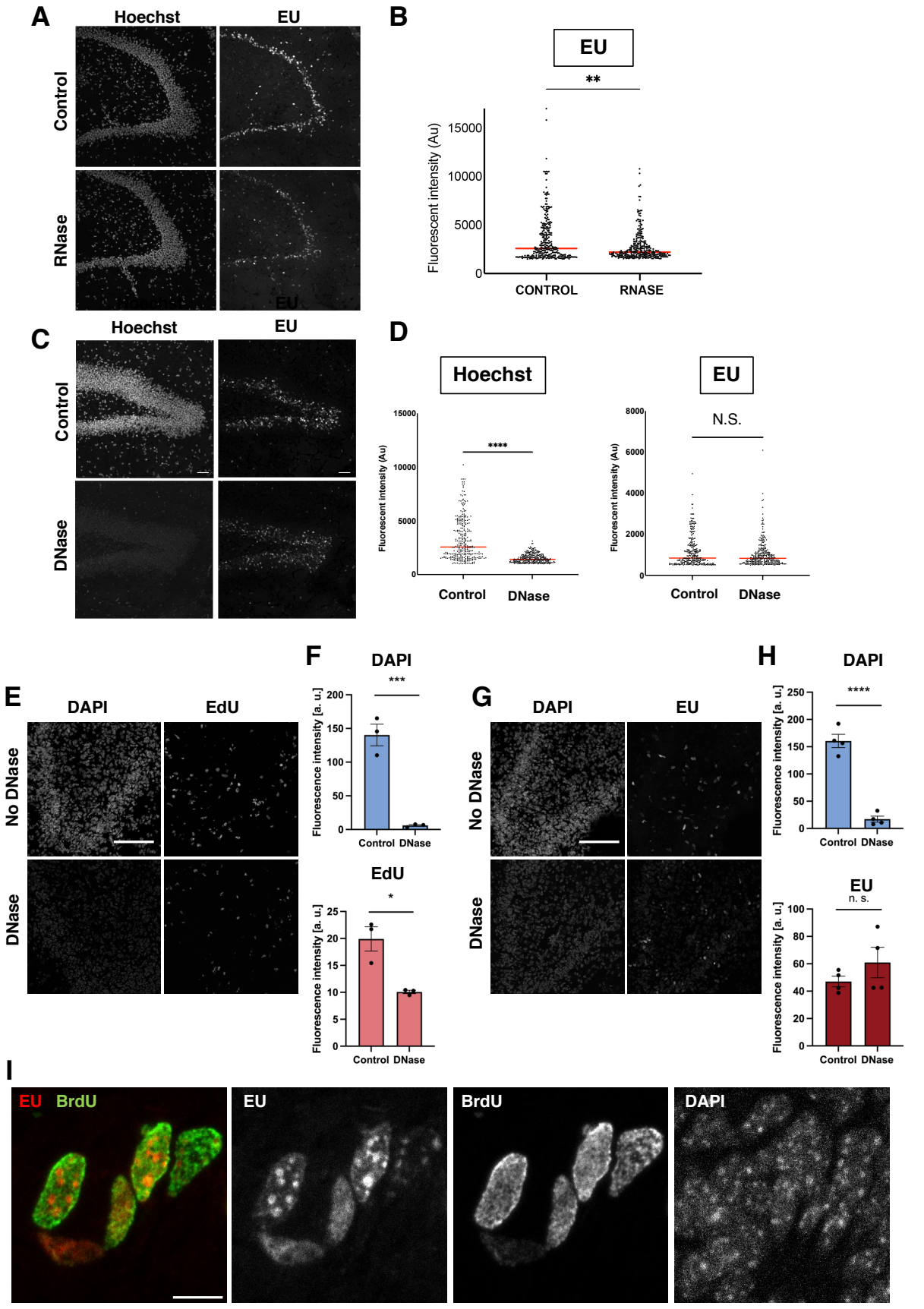
A
Hoechst
EU
Control
RNase
B
EU
**
Fluorescent intensity (Au)
15000
10000
5000
0
CONTROL
RNASE
C
Hoechst
EU
Control
DNase
D
Hoechst
EU
****
N.S.
Fluorescent intensity (Au)
Control
DNase
E
DAPI
EdU
No DNase
DNase
F
DAPI
***
Fluorescence intensity [a. u.]
Control DNase
EdU
*
G
DAPI
EU
H
DAPI
****
EU
n. s.
I
EU BrdU
EU
BrdU
DAPI

Fig. S5.

RNase-sensitive but not DNase-sensitive EU signals in brain tissues. (A-B) EU signals in the DG are reduced by RNase treatment. $^{**}P < 0.01$ (Mann-Whitney test). (**C-D**) DNase I treatment extinguishes Hoechst signals of individual nuclei but not EU signals. $^{****}P < 0.0001$, N.S. not significant (Mann-Whitney test). (**E-H**) Validation that DNase I treatment reduces EdU signals, which integrate into DNA, but not EU signals, further confirming specific EU labeling. EdU or EU were injected into P3 mice and brain tissue was harvested 4 h after injection. EdU and EU visualization were performed in parallel using identical staining protocols. Quantification in F, H compares total signal intensities in the DG from n = 3-4 experiments (unpaired *t*-test; $^{****}P < 0.0001$, $^{***}P < 0.001$, $^{*}P < 0.05$, n.s. not significant). (**I**) Distinct nuclear localization of EU and BrdU signals further suggests RNA-specific EU labeling. EU and BrdU were injected at the same time in P3 mice and brain tissue was harvested 4 h after injection. Scale bars, 100 μm in A, C, E, G; 10 μm in I.

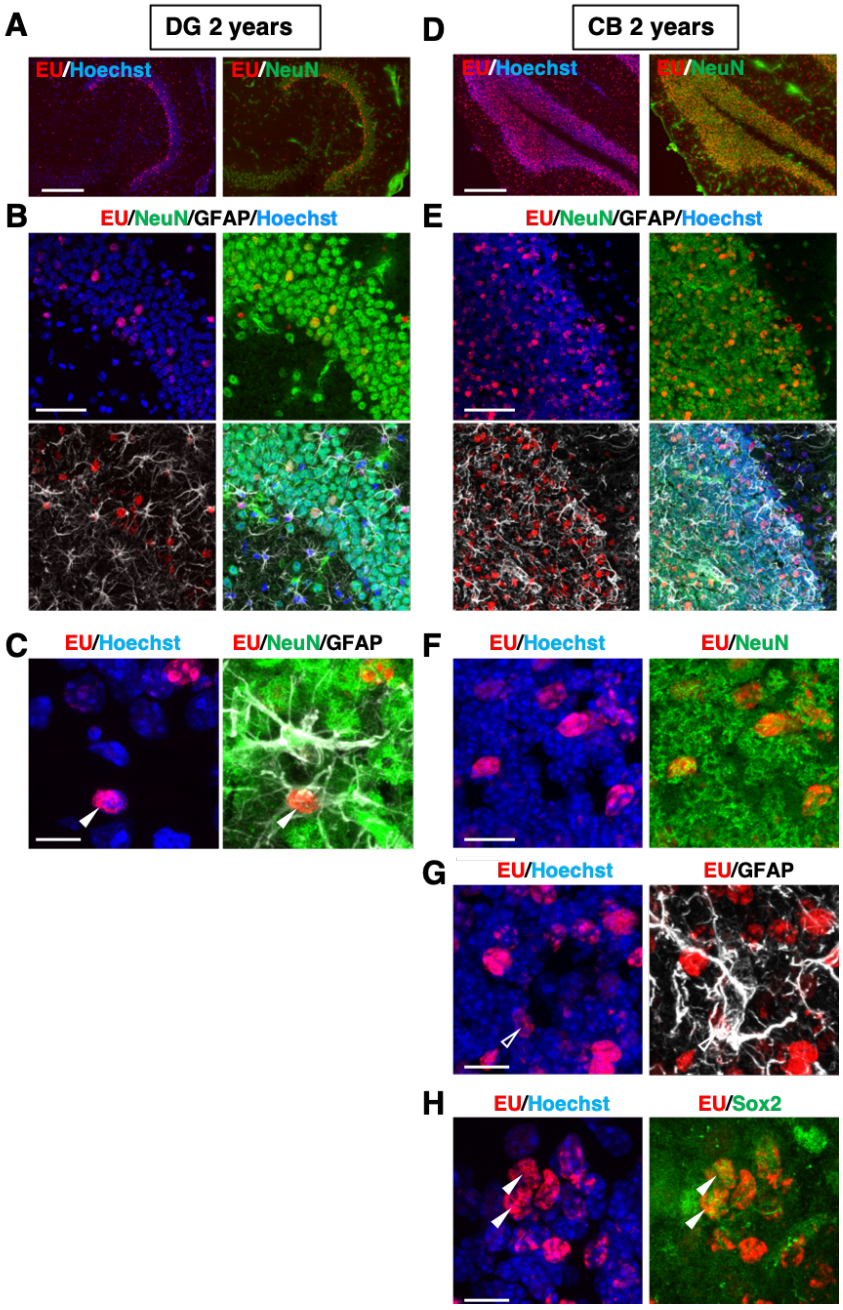

Fig. S6.

Distribution of EU$^+$ cells in 2-year-old brains. (**A-C**) Distribution of EU$^+$ cells in the DG. The majority of EU signals resided in the dentate granule cell layer 2 years after EU injections. (**B** and **C**) Higher magnification images. The majority of EU signals colocalized with NeuN (B) but EU$^+$/GFAP$^+$ cells (arrowhead) were also found (**C**). (**D-H**) Distribution of EU$^+$ cells in the CB. The majority of EU signals resided in the granule layer of CB 2 years after EU injections. (**E, F, G** and **H**) Higher magnification images. Colocalization of EU signals with NeuN$^+$ cells (F) and GFAP$^+$ cells (G, open arrowhead) in the granule cell layer, and Sox2$^+$ cells (H, arrowheads) between the granule layer and the molecular layers. Scale bars, 250 μm (A, D), 50 μm (B, E), and 10 μm (C, F, G, and H).

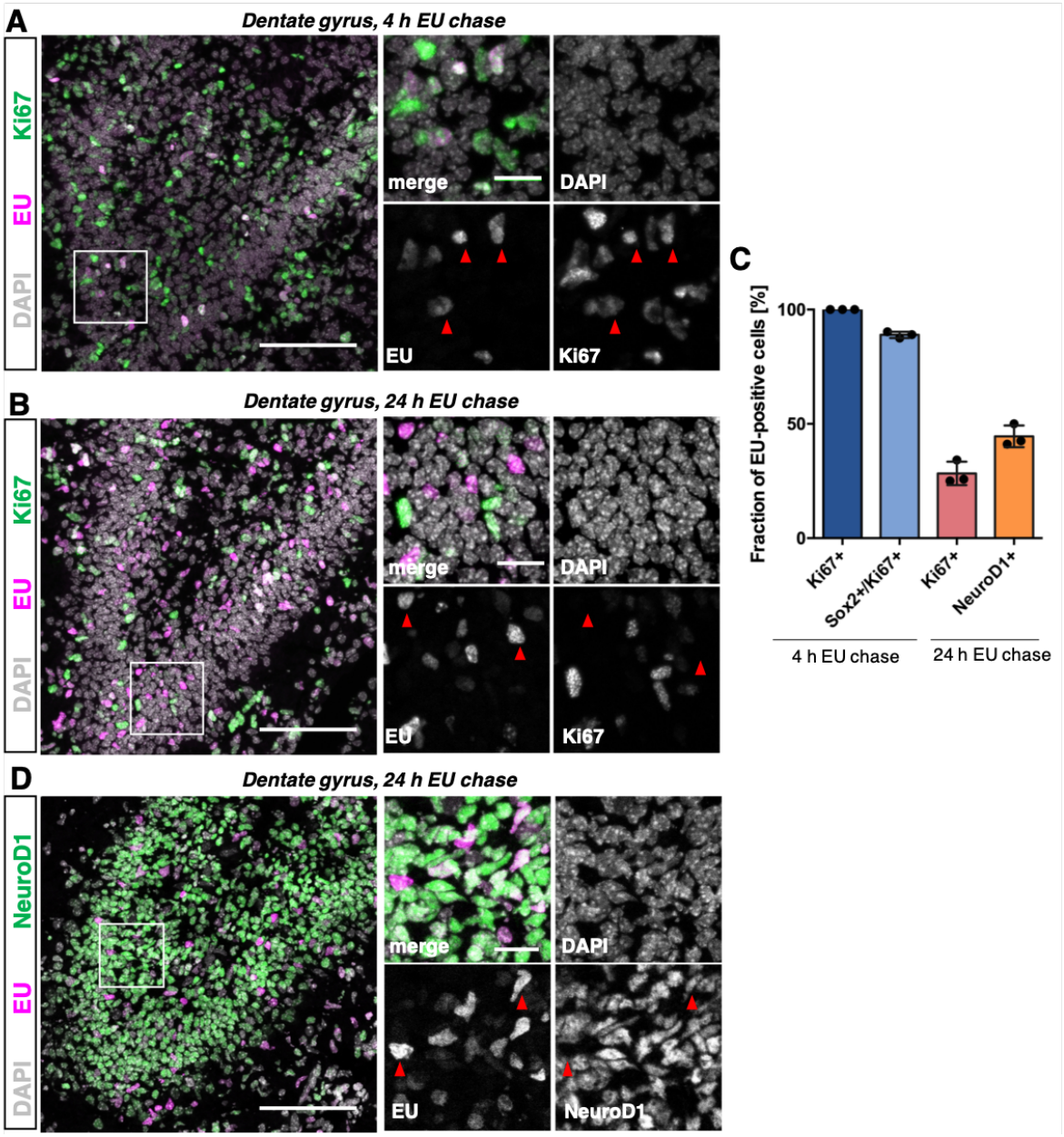

Fig. S7.

Long-term retention of RNA in the hippocampus is correlated with cell cycle exit during neurogenesis. (**A**) At 4 h after EU injection into P3 mice, all EU^+ cells in the hippocampus co-localized proliferation marker Ki67. (**B**) Only a subset of EU^+ cells expressed Ki67, when EU was injected daily from P3-5 and brains analyzed at P6 (24 h after the last injection). (**C**) Cell type quantifications (n=3 mice). Shown are individual data points with means ± SEM. (**D**) Half of the EU^+ cells expressed neuronal commitment and differentiation marker NeuroD1 when EU was injected daily from P3-5, and brains were analyzed at P6 (24 h after the last injection). Scale bars are 100 µm in low magnification images and 20 µm in high magnification images. Small white boxes in A, B, D are magnified on the right side.

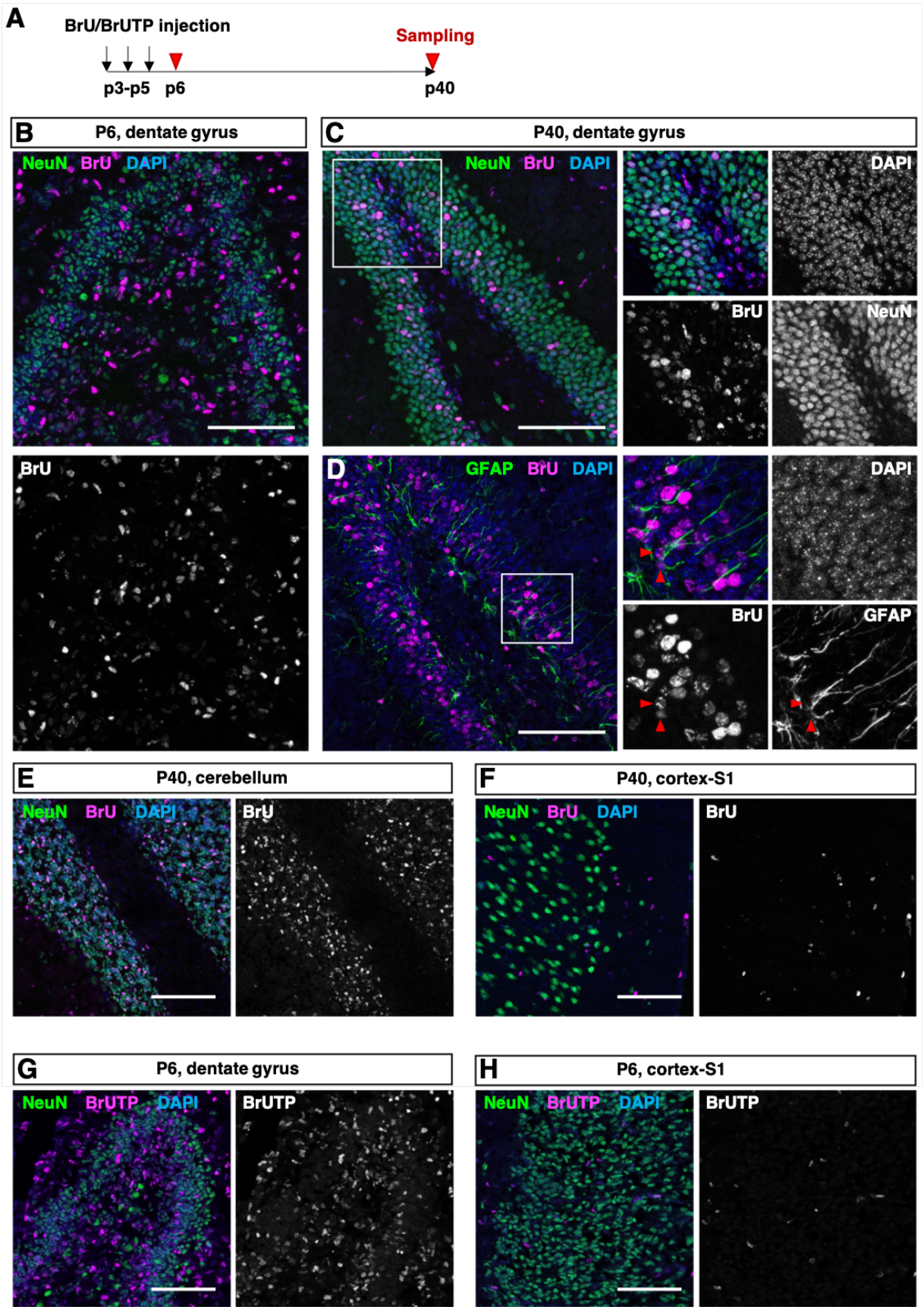
A
BrU/BrUTP injection
Sampling
p3-p5
p6
p40
B
P6, dentate gyrus
NeuN BrU DAPI
BrU
C
P40, dentate gyrus
NeuN BrU DAPI
DAPI
BrU
NeuN
D
GFAP BrU DAPI
DAPI
BrU
GFAP
E
P40, cerebellum
NeuN BrU DAPI
BrU
F
P40, cortex-S1
NeuN BrU DAPI
BrU
G
P6, dentate gyrus
NeuN BrUTP DAPI
BrUTP
H
P6, cortex-S1
NeuN BrUTP DAPI
BrUTP

Fig. S8.

Distributions of BrU label-retaining cells in the mouse brain. (**A**) Experimental scheme. Mice received daily injections of either BrU (B-F) or BrUTP (G-H) on P3-P5 and were analyzed one day or one month after the last injection (P6 and P40). BrU/BrUTP$^+$ cells were visualized by immunohistochemistry. (**B**) Distribution of BrU$^+$ cells in the dentate gyrus at P6. (**C**) Most BrU$^+$ cells at P40 in the dentate gyrus co-localize neuronal marker NeuN. (**D**) BrU label can also be found in GFAP-positive ANPCs with radial glia-like morphology in the subgranular zone. Red arrows highlight nuclei of radial glia. Small boxes in C,D were magnified on the right side.
(**E**) BrU signal in the cerebellum at P40. (**F**) Only few cells in the cortex retained BrU signals at P40. (**G-H**) Similar as observed after EU and BrU injections, dense BrUTP-label retaining cells were observed in the dentate gyrus but not in the cortex of P6 mice. Scale bars in B-H: 100 µm.

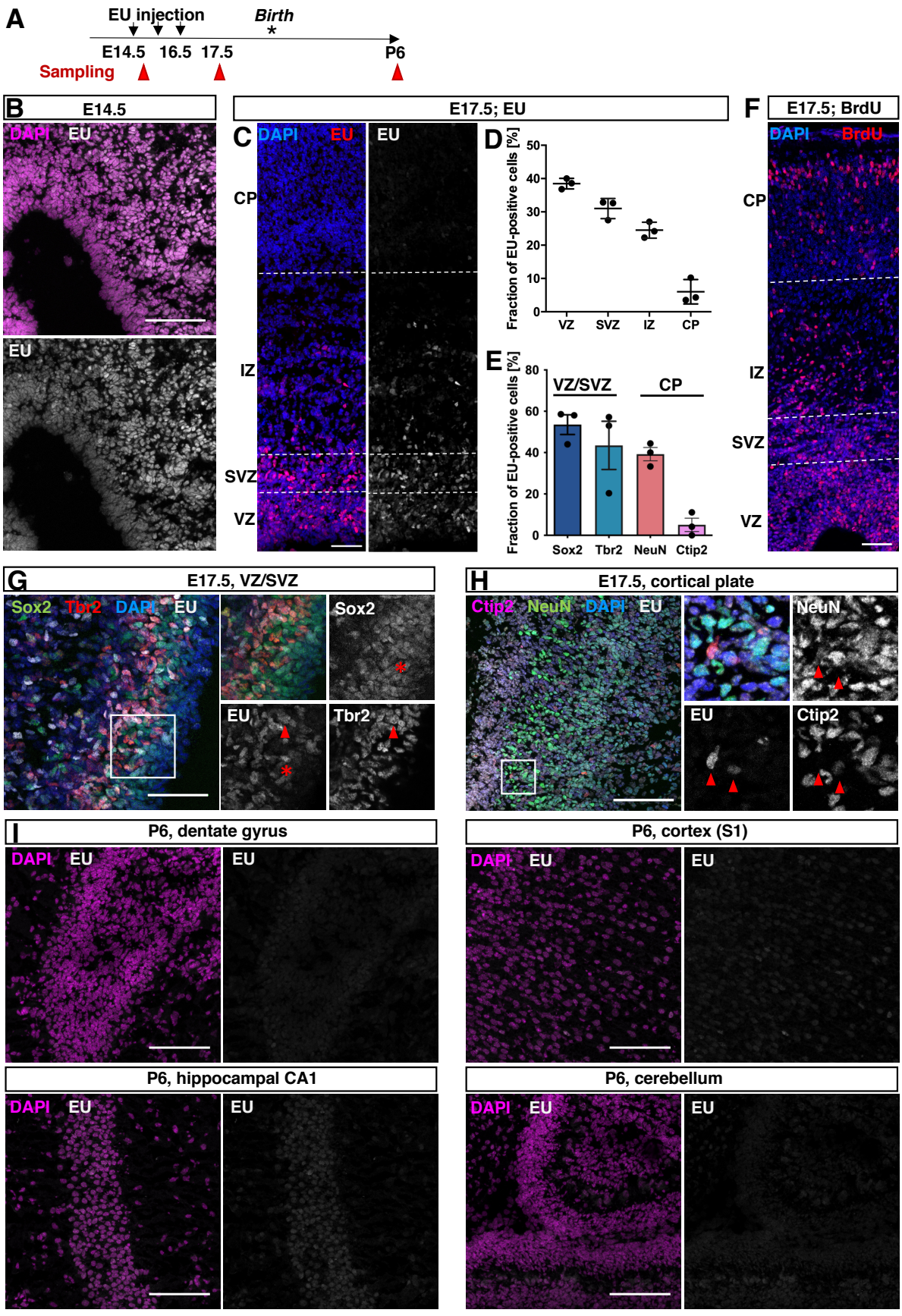
A
EU injection
Birth
E14.5
16.5
17.5
P6
Sampling
B
E14.5
DAPI
EU
EU
C
E17.5; EU
DAPI
EU
EU
CP
IZ
SVZ
VZ
D
Fraction of EU-positive cells [%]
VZ
SVZ
IZ
CP
E
Fraction of EU-positive cells [%]
VZ/SVZ
CP
Sox2
Tbr2
NeuN
Ctip2
F
E17.5; BrdU
DAPI
BrdU
CP
IZ
SVZ
VZ
G
E17.5, VZ/SVZ
Sox2
Tbr2
DAPI
EU
Sox2
EU
Tbr2
H
E17.5, cortical plate
Ctip2
NeuN
DAPI
EU
NeuN
EU
Ctip2
I
P6, dentate gyrus
DAPI
EU
EU
P6, cortex (S1)
DAPI
EU
EU
P6, hippocampal CA1
DAPI
EU
EU
P6, cerebellum
DAPI
EU
EU

Fig. S9.

Limited retention of embryonically generated RNA. (**A**) Experimental scheme for EU injection and sample collection. (**B**) Ubiquitous EU signal in the neocortex at 1 h after EU injection into pregnant dams. (**C-D**) Distribution of EU^+ cells in the embryonic cortex at E17.5 (24 h after the last EU injection). CP, cortical plate; IZ, intermediate zone; SVZ, subventricular zone; VZ, ventricular zone. (**E**) Percentage of EU^+ cells that co-localize NSC marker Sox2 or intermediate progenitor marker Tbr2 in the VZ/SVZ and neuronal markers Ctip2 or NeuN in the CP. Data in D, E represent individual embryos with mean +/- SEM. (**F**) Distribution of $BrdU^+$ cells in the embryonic cortex at E17.5 representing cortical neurogenesis. BrdU was injected at E14.5 and E16.5. (**G**) Representative fluorescent image depicting EU/$Sox2^+$ cells (asterisk) and EU/$Tbr2^+$ cells (arrowhead) in the neocortex. (**H**) Fluorescent image of the CP showing that most EU^+ cells do not express Ctip2 or NeuN. Scale bars in B, 100 μm; in C-H, 50 μm. Small boxes in G,H are magnified on the right side. (**I**) No clear EU signals can be observed in the mouse brain at P6 when EU was injected daily at E14.5-E16.5. Scale bar in I, 100 μm.

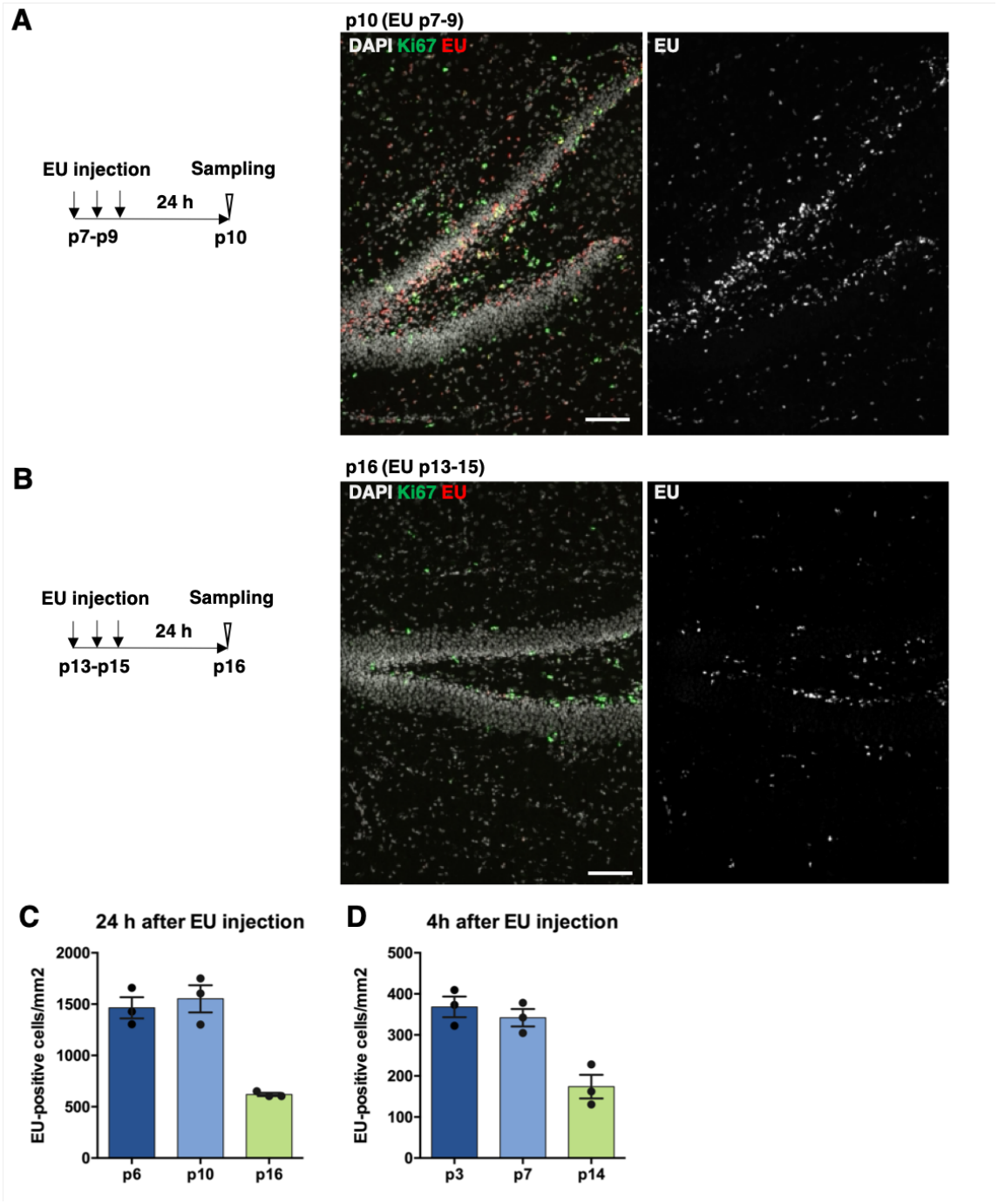

Fig. S10.

EU label-retaining cells in the hippocampus of 1-week-old mice and 2-week-old mice. (**A**) Dense EU label was observed in the hippocampus of 1-week-old mice when EU was injected P7-P9 and analyzed at P10. (**B**) Sparse EU label was observed in 2-week-old mice when EU was injected P13-P15 and analyzed at P16. (**C**) While the density of EU^+ cells in the dentate gyrus did not differ between P6 and P10 (*t*-test, $P = 0.63$), it was reduced at P16 compared to P10 (*t*-test, $P = 0.0022$). (**D**) The reduction in EU-label retaining cells in 2-week-old mice was already apparent when EU^+ cells were quantified at 4 h after a single EU injection. Scale bars, 100 µm.

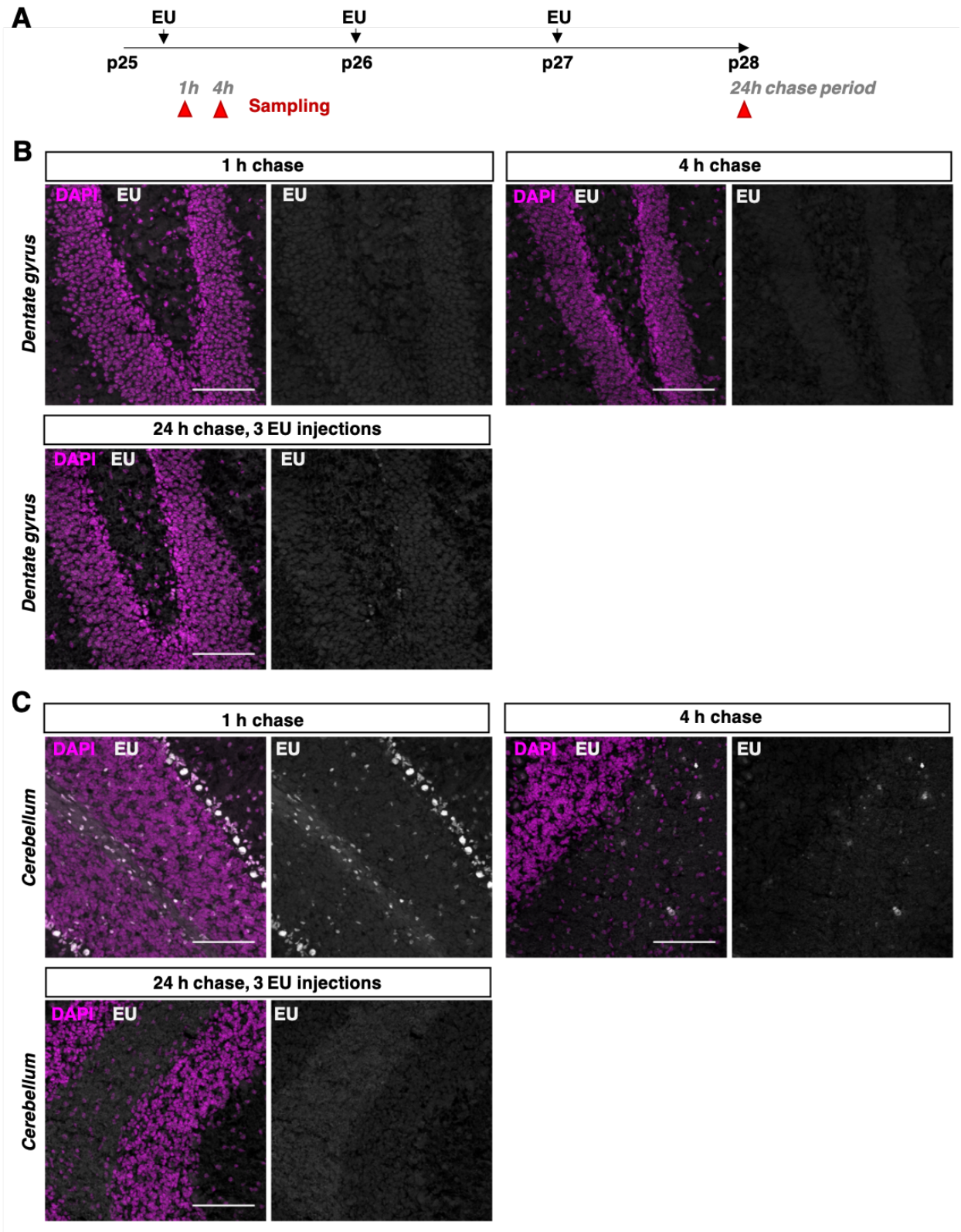
A
EU
EU
EU
p25
p26
p27
p28
1h
4h
Sampling
24h chase period
B
1 h chase
4 h chase
DAPI
EU
EU
Dentate gyrus
24 h chase, 3 EU injections
C
Cerebellum

Fig. S11.

Limited RNA labeling by EU in the brain of 4-week-old mice. (**A**) Experimental scheme. EU was injected daily at P23-P25 and mice were analyzed at 1 h or 4 h after a single EU injection or 24 h after the last EU injection (P27). (**B**) No clear EU signal in the hippocampus at 1 h, 4 h or 24 h after EU injection. (**C**) Isolated cells in the cerebellum were EU-positive at 1 h after injection, but this signal was not maintained long-term. Scale bars, 100 μm.

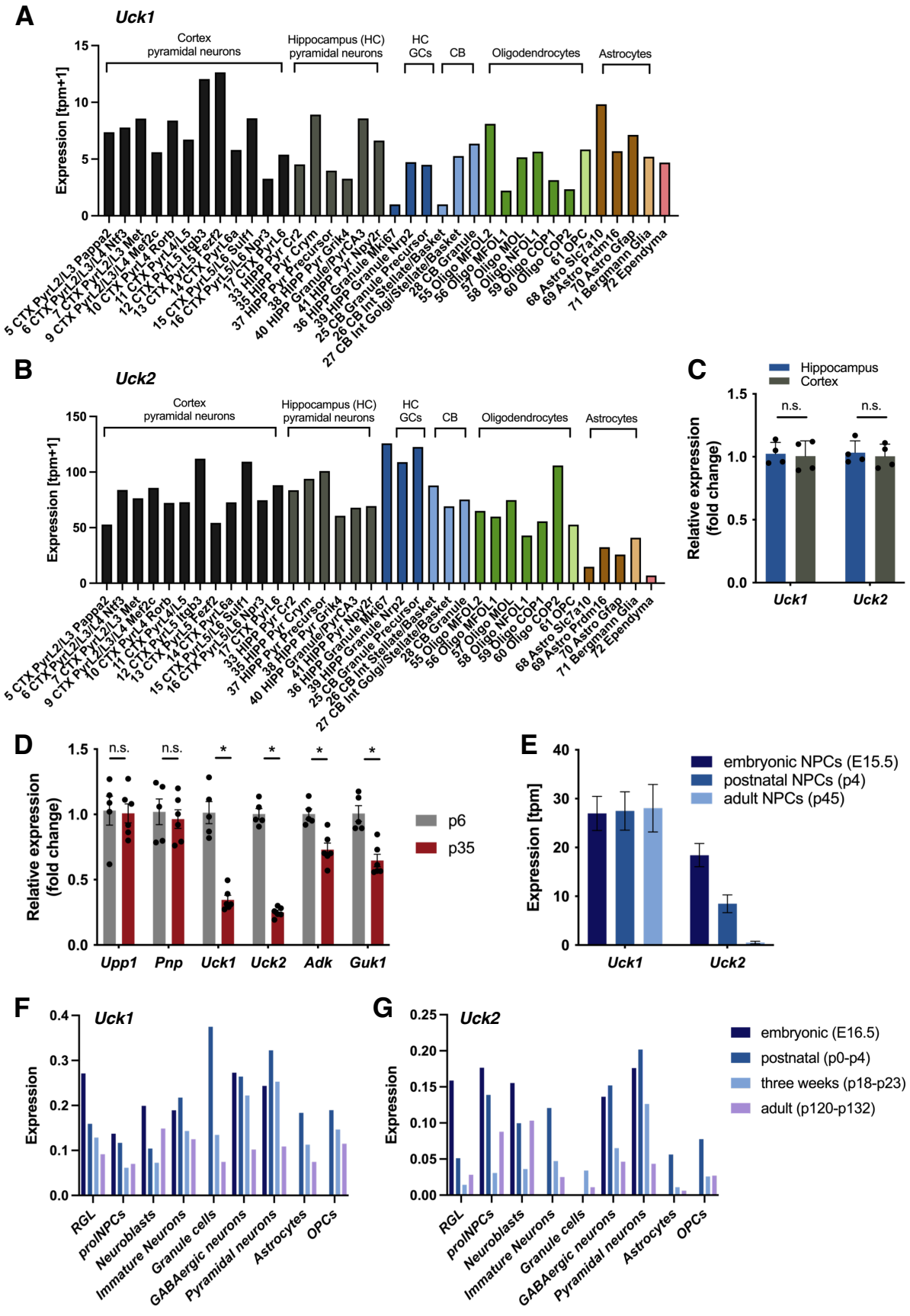
A
Uck1
Expression [tpm+1]
Cortex pyramidal neurons
Hippocampus (HC) pyramidal neurons
HC GCs
CB
Oligodendrocytes
Astrocytes
B
Uck2
C
Hippocampus
Cortex
Relative expression (fold change)
n.s.
Uck1
Uck2
D
p6
p35
Upp1
Pnp
Uck1
Uck2
Adk
Guk1
E
embryonic NPCs (E15.5)
postnatal NPCs (p4)
adult NPCs (p45)
Expression [tpm]
F
Uck1
Expression
RGL
proINPCs
Neuroblasts
Immature Neurons
Granule cells
GABAergic neurons
Pyramidal neurons
Astrocytes
OPCs
G
Uck2
embryonic (E16.5)
postnatal (p0-p4)
three weeks (p18-p23)
adult (p120-p132)

Fig. S12.

Expression of pyrimidine salvage pathway enzymes in the mouse brain. (A-B) Uridine-cytidine kinases *Uck1* and *Uck2* are expressed in different cell types of the postnatal brain. Data are depicted as transcript per million (tpm) per cell cluster from single-cell RNA sequencing of the whole mouse brain (P2 and P11) derived from Rosenberg *et al* (*34*). Cell clusters are labelled according to their original naming in Rosenberg *et al*. **(C)** The expression of *Uck1* and *Uck2* does not differ between hippocampus and cortex tissue in postnatal mice (P6) as assessed by qRT-PCR. n. s. - not significant, unpaired *t*-test, n = 4 mice. **(D**) Age-dependent reduction in the expression of salvage pathway-related genes in the hippocampus between P6 and P35 as shown by qRT-PCR. $*P < 0.05$ (unpaired *t*-test, n = 5-6 mice). **(E**) Age-dependent reduction in Uck1 and Uck2 expression in hippocampal NPCs. Data derived from RNA sequencing of FACS-purified NPC populations retrieved from Berg *et al* (*35*). **(F-G**) Age-dependent reduction in *Uck1* and *Uck2* expression in different hippocampal cell types. Data are derived from single-cell RNA sequencing analysis of the developing hippocampus published in Hochgerner *et al* (*36*). Note that no granule cells, astrocytes and oligodendrocyte progenitor cells (OPCs) were detected in the embryonic brain.

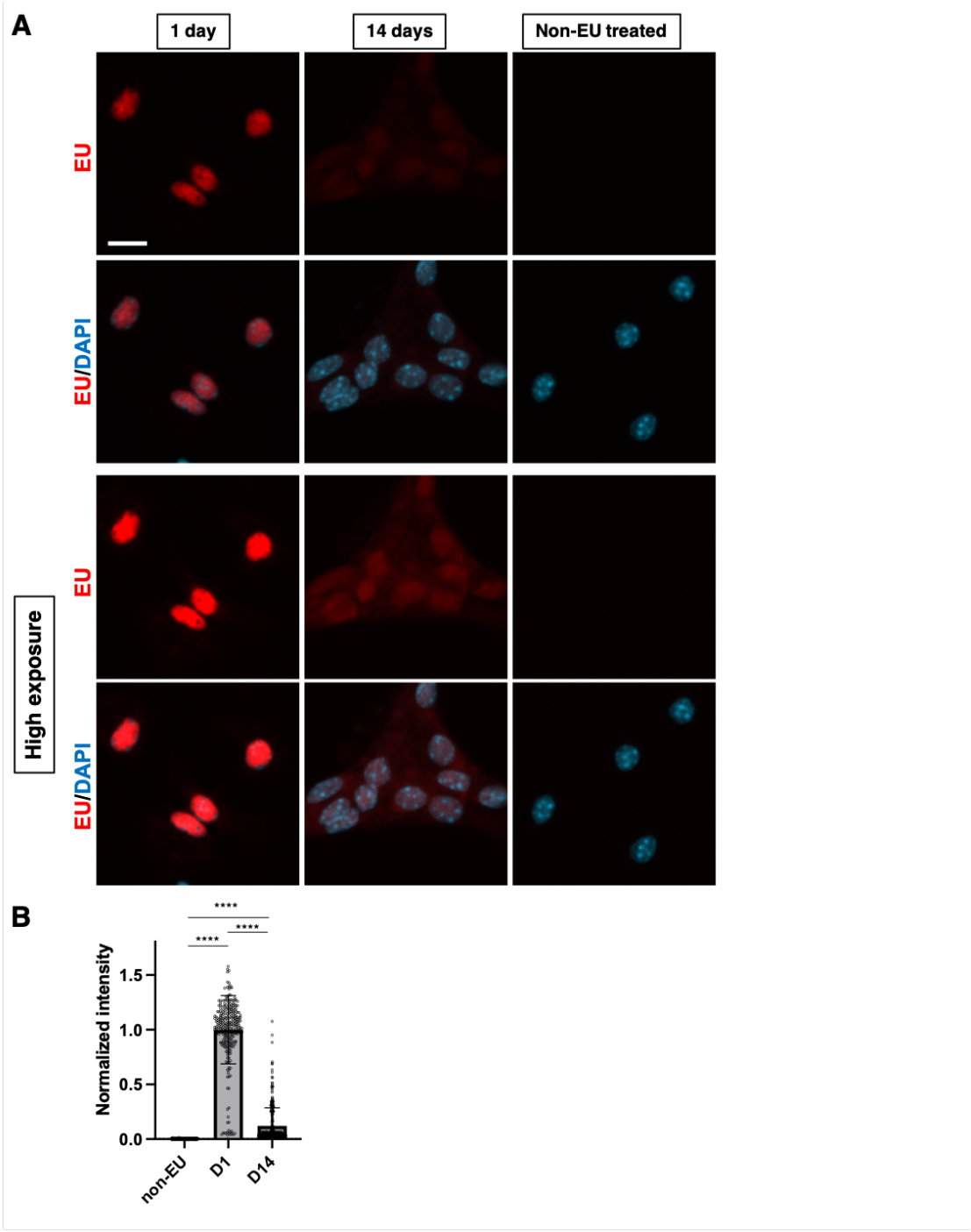

Fig. S13.

Two weeks' retention of EU signals in quiNPCs *in vitro*. Cells were labelled with EU at day 1 and day 2 after induction of quiescence and EU-label retention was analyzed two weeks later. (**A**) Representative fluorescent images of EU staining after acute (24 h) EU labelling and at 14 d after EU labelling. Scale bar, 10 µm. (**B**) Quantification of EU fluorescent intensities. Depicted are normalized intensities of individual nuclei with means ± SEM. ****$P < 0.0001$ from Kruskal Wallis test with post hoc Dunn's test.

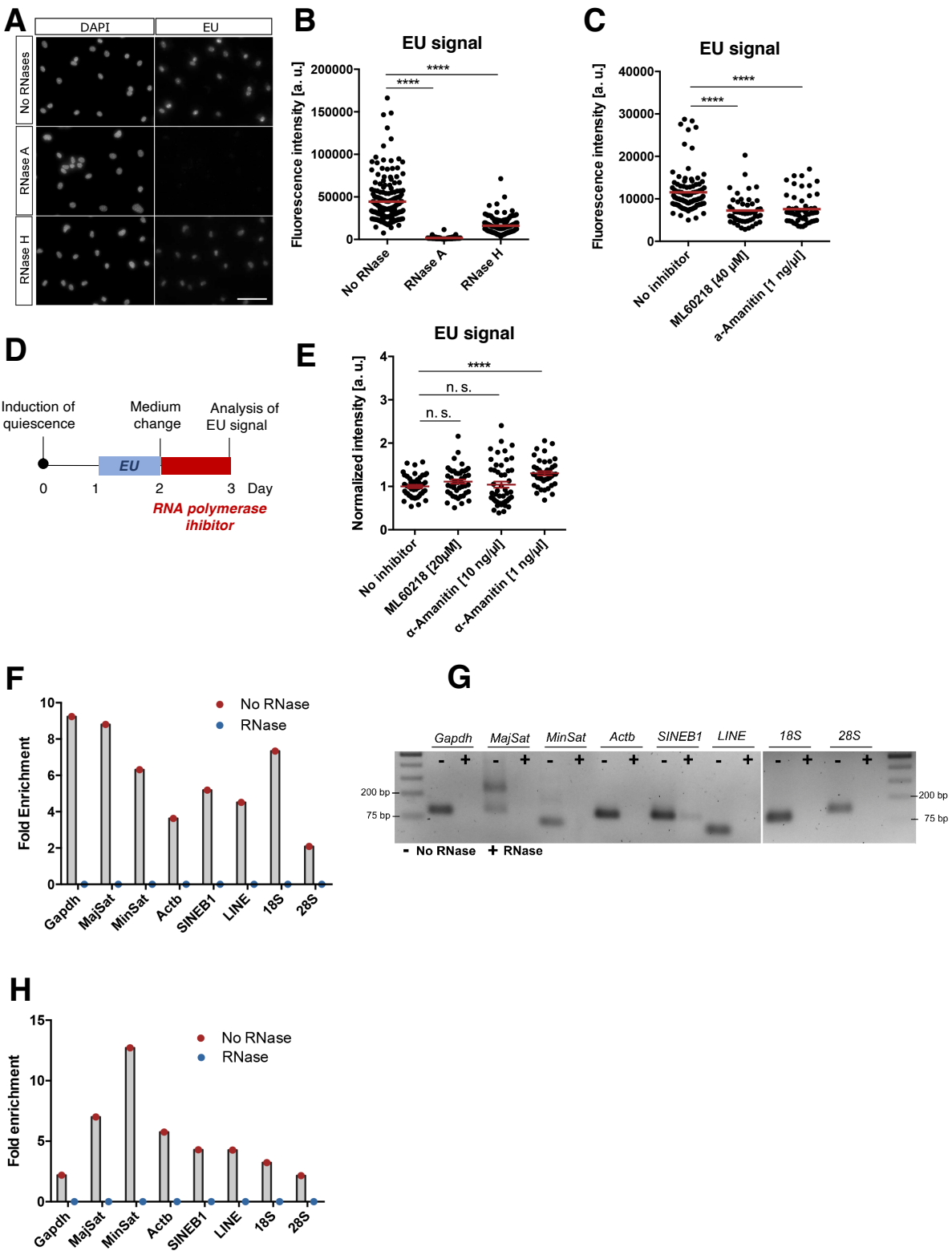
A
DAPI
EU
No RNases
RNase A
RNase H
B
EU signal
Fluorescence intensity [a. u.]
200000
150000
100000
50000
0
****
****
No RNase
RNase A
RNase H
C
EU signal
Fluorescence intensity [a. u.]
40000
30000
20000
10000
0
****
****
No inhibitor
ML60218 [40 µM]
a-Amanitin [1 ng/µl]
D
Induction of quiescence
Medium change
Analysis of EU signal
EU
0
1
2
3
Day
RNA polymerase ihibitor
E
EU signal
Normalized intensity [a. u.]
4
3
2
1
0
****
n. s.
n. s.
No inhibitor
ML60218 [20µM]
α-Amanitin [10 ng/µl]
α-Amanitin [1 ng/µl]
F
Fold Enrichment
10
8
6
4
2
0
No RNase
RNase
Gapdh
MajSat
MinSat
Actb
SINEB1
LINE
18S
28S
G
Gapdh
MajSat
MinSat
Actb
SINEB1
LINE
18S
28S
- + - + - + - + - + - + - + - +
200 bp
75 bp
200 bp
75 bp
- No RNase + RNase
H
Fold enrichment
15
10
5
0
No RNase
RNase
Gapdh
MajSat
MinSat
Actb
SINEB1
LINE
18S
28S

Fig. S14.

Depletion of EU signals by RNase treatment in quiNPCs. (**A**) Treatment of fixed cells with RNase A and RNase H abolishes EU signals in quiNPCs. Scale bar, 50 µm. (**B**) Quantification of EU signals after RNase treatments. ****$P < 0.001$ from Mann-Whitney test. (**C**) Treatment of quiNPCs with ML60218, an inhibitor of RNA polymerase III, or with RNA polymerase II inhibitor alpha-Amanitin before and during incubation with EU significantly reduces EU signals ****$P < 0.001$ from Mann-Whitney test. (**D**) Experimental scheme for E. NPCs were labelled with EU on day 1 after induction of quiescence. On day 2, EU was washed out and cells were cultured in the presence of RNA polymerase inhibitors alpha-amanitin and ML60218. Incubation of quiNPCs for longer periods after EU administration in the presence of RNA polymerase inhibitors led to cell death. (**E**) Quantification of EU signal intensities in quiNPCs. Represented are normalized signal intensities for each nucleus with mean ± SEM for each group (n = 2). (**F**) RNase treatment depletes the enrichment of repeat RNAs in EU-labelled nucleic acids isolated from quiNPCs. (**G**) Representative agarose gel shows abolished PCR products after RNase treatment of quiNPC RNA. (**H**) RNase treatment depletes the enrichment of repeat RNAs in EU-labelled nucleic acids isolated from the CB.

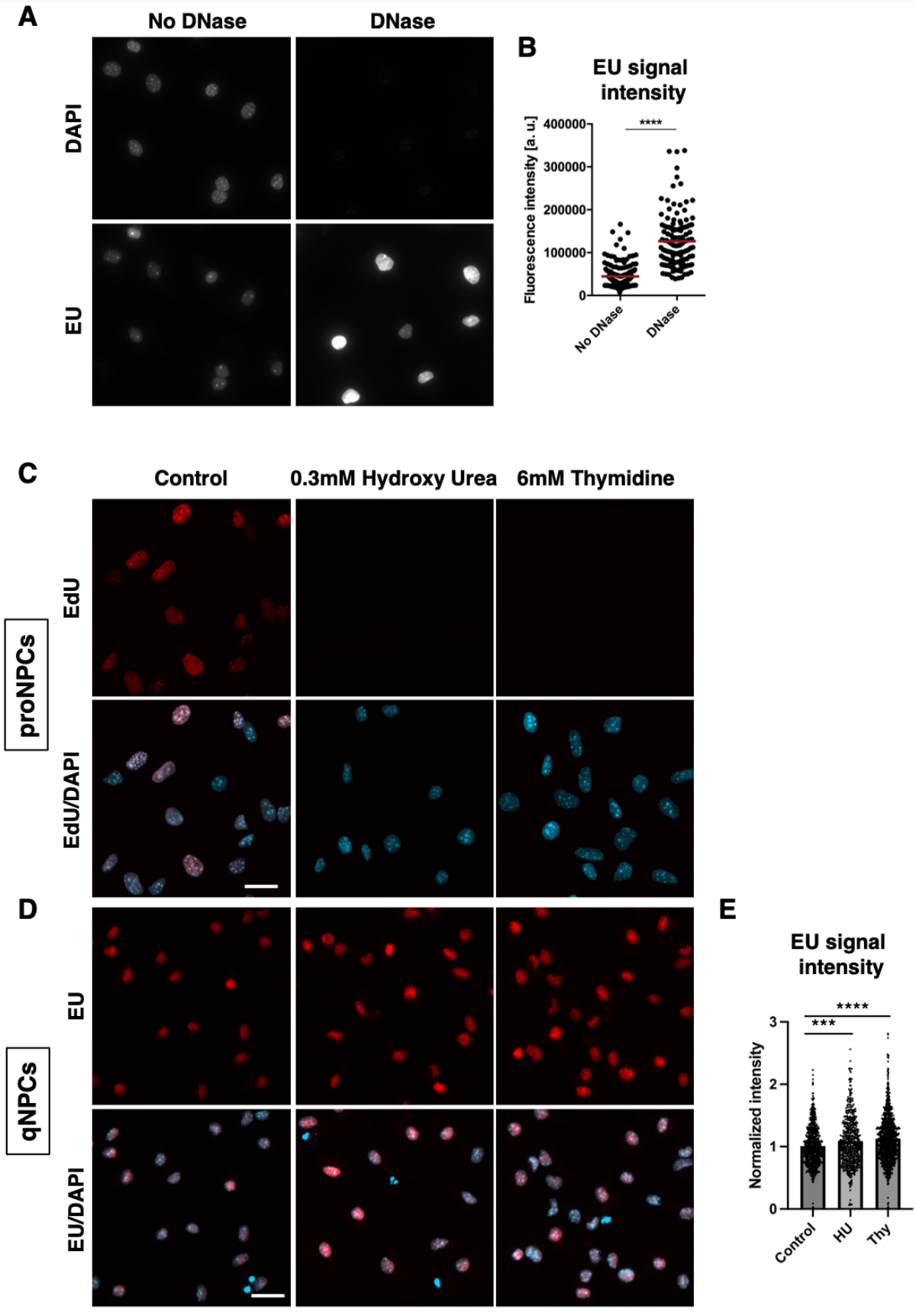
A
No DNase
DNase
DAPI
EU
B
EU signal intensity
Fluorescence intensity [a. u.]
400000
300000
200000
100000
0
****
No DNase
DNase
C
Control
0.3mM Hydroxy Urea
6mM Thymidine
proNPCs
EdU
EdU/DAPI
D
qNPCs
EU
EU/DAPI
E
EU signal intensity
Normalized intensity
3
2
1
0
***
****
Control
HU
Thy

Fig. S15.

Supporting evidence that EU signals in quiNPCs are not derived from incorporation into genomic DNA. (**A**) Treatment of fixed EU-labelled quiNPCs with DNase I depleted DAPI signal but did not abolish EU signals. Higher EU signal intensities after DNase treatment are presumably due to increased staining accessibility of nuclear RNA. (**B**) Quantification of EU signal intensities in quiNPCs with and without DNase I digest. Represented are signal intensities for each nucleus with group means (****$P < 0.0001$, unpaired *t*-test). (**C**) Ribonucleotide reductases convert ribonucleotides into deoxyribonucleotides, which is required for integration into DNA. Treatment of proliferating NPCs (ProNPCs) with ribonucleotide reductase inhibitors hydroxy urea (HU) and thymidine (Thy) abolished EdU signals. (**D-E**) Treatment of quiNPCs with ribonucleotide reductase inhibitors did not reduce EU signal intensities. Depicted are normalized intensities for individual nuclei with group means. Scale bars in C, D: 20 µm. ***$P < 0.001$, **** $P < 0.0001$, Kruskal-Wallis test followed by Dunn's multiple comparisons test.

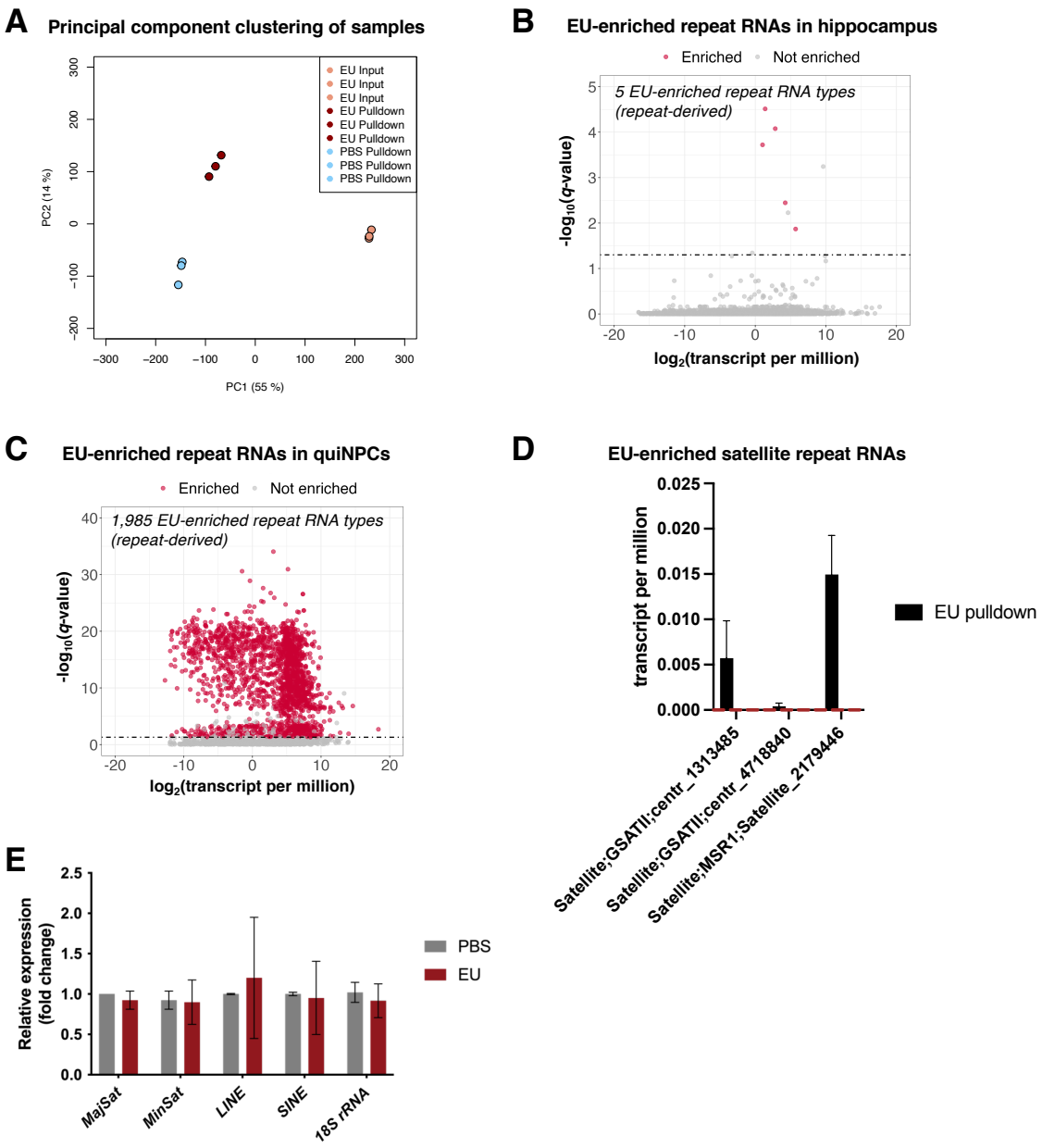

Fig. S16.

Supplementary information related to composition of EU-enriched RNA. (**A**) PCA plot showing separation of EU-RNA-Sequencing samples from quiNPCs based on mapping to mm39. (**B-C**) MA plots depicting long-retained repeat RNAs (EU-enriched; Wald test, q-value < 0.05 and b > 0) in the hippocampus (B) and in quiNPCs *in vitro* (C). (**D**) Long-retained EU transcripts in quiNPCs contain *satRNAs*. Depicted are mean transcript per million (tpm) in EU-pulldown compared to non-EU-pulldown samples (red line depicts tpm of 0 in PBS-treated quiNPCs). (**E**) EU treatment does not affect repeat RNA levels in quiNPCs compared to PBS-treated quiNPCs as assessed by qRT-PCR (t-test: $P > 0.05$ for each repeat RNA; n = 4 per group).

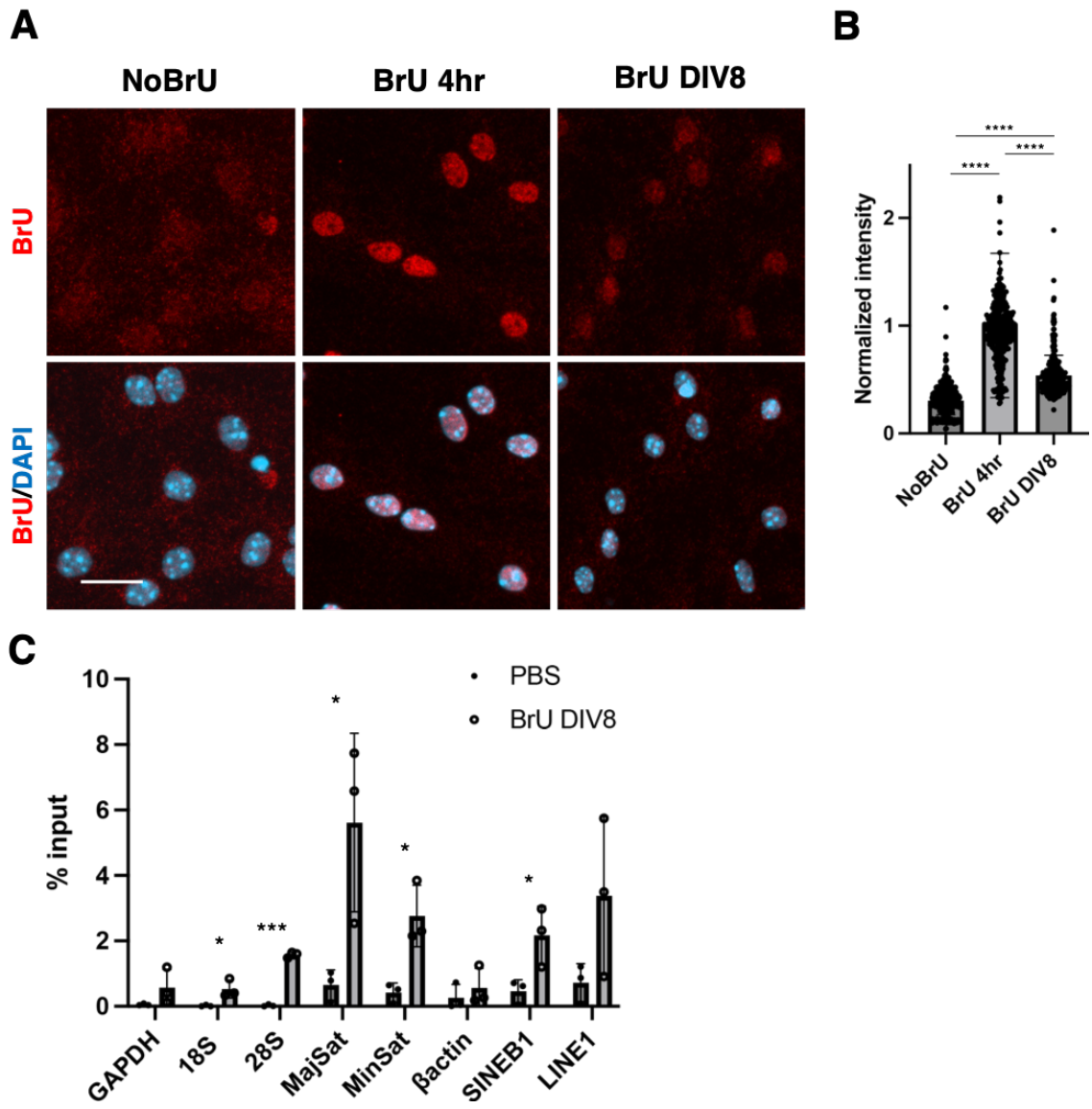

Fig. S17.

BrU label retention in quiescent NPCs. (**A**) BrU was applied to quiNPCs on days 1 and 2 after induction of quiescence. Immunofluorescent signals against BrU in non-treated cells, quiNPCs 4 h after BrU addition, and 8 days after BrU treatment (DIV8). Retention of BrU signals in nuclei was observed at DIV8. Scale bar, 20 µm. (**B**) Quantification of BrU signal intensities. Kruskal-Wallis test, followed by Dunn's multiple comparisons. (****$P < 0.0001$, Kruskal-Wallis test) (**C**) BRIC-qPCR on BrU-labelled quiNPCs. RNA was isolated from quiNPCs 8 days after BrU treatment. BrU-labelled transcripts were pulled down and enrichment of specific transcripts was measured by qRT-PCR (n = 3 independent experiments, *t*-test *$P < 0.05$; ***$P < 0.001$).

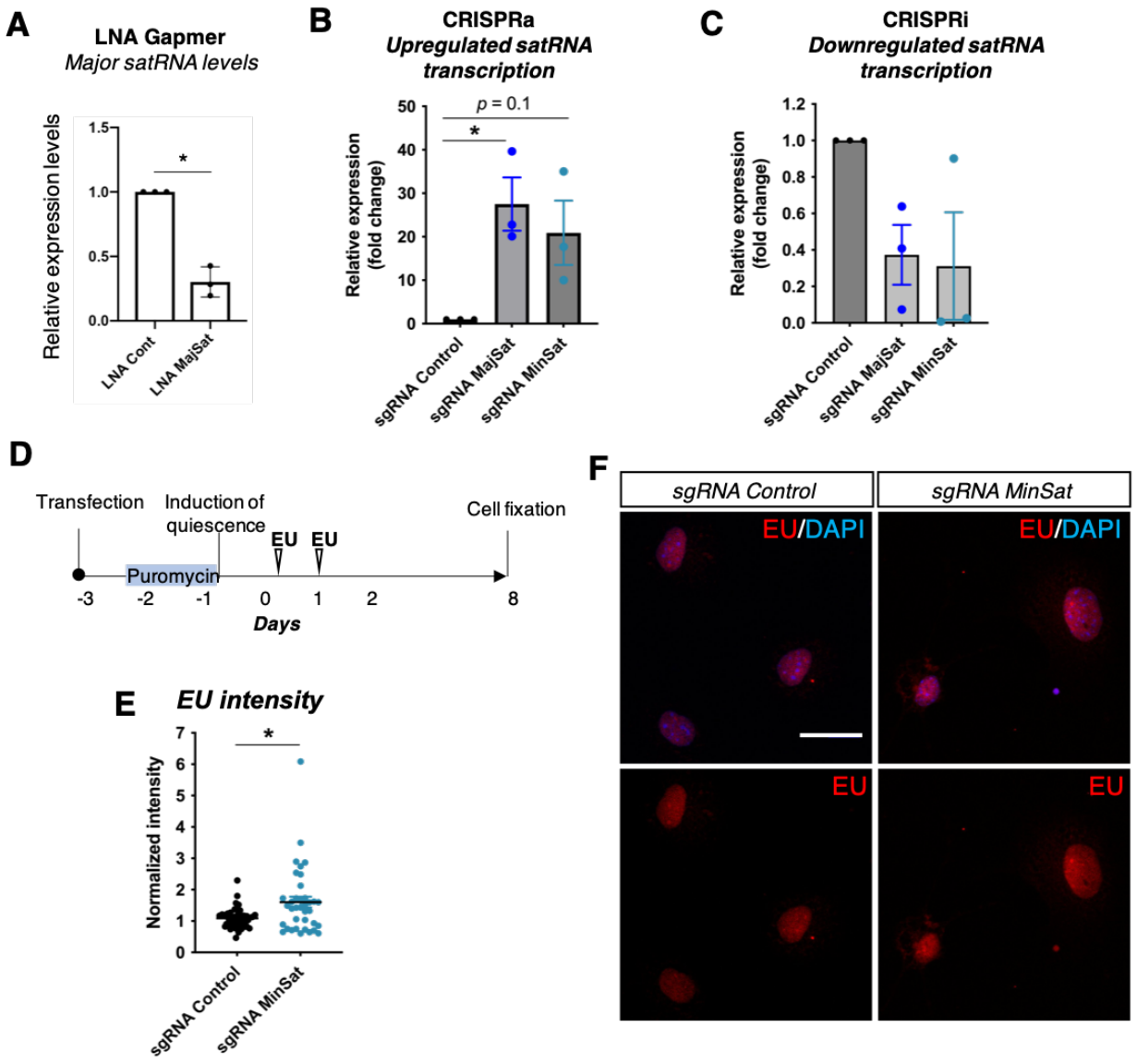

Fig. S18.

Manipulation of *satRNA* levels in NPCs. (**A**) LNA-mediated knock-down of *major satRNAs* in NPCs measured by qRT-PCR. One-sample *t*-test, **P* < 0.05. (**B**) CRISPRa-based activation of *major* and *minor satRNA* expression. NPCs were transfected with sgRNA targeting major and minor satellite repeats and dCas9-VPR constructs. *Major* and *minor satRNA* expression was assessed by qRT-PCR on day 3 after transfection. One-sample *t*-test, **P* < 0.05. (**C**) CRISPRi-based transcriptional repression of *major* and *minor satRNAs*. NPCs were transfected with sgRNA and dCas9-KRAB constructs and expression was assessed 5 days after transfection. (**D**) Experimental scheme for results depicted in E-F. (**E-F**) Overexpression of *minor satRNAs* increases EU signal retention. **P* < 0.05 (Mann Whitney test; depicted are individual nuclei from 3 experiments). Scale bar, 20 µm. Note that the experiment depicted in Fig. S18D-F was performed at the same time as the experiment depicted in Fig. 3H-I and sgRNA MinSat and sgRNA MajSat were compared to the same control (sgRNA Control). Thus, EU intensities and the representative image for sgRNA control depicted in Fig. S18E-F are identical to Fig. 3H-I.

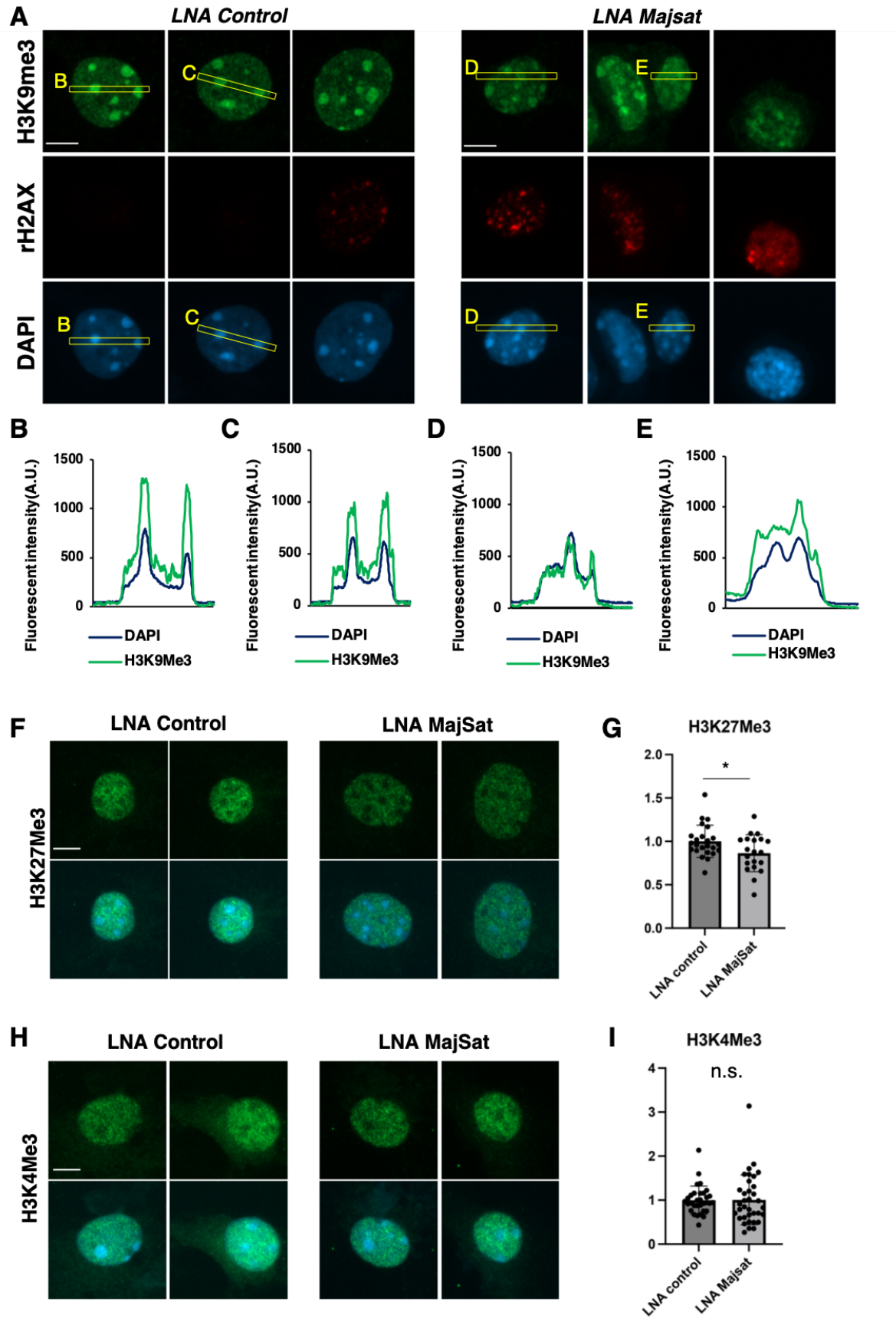
A
LNA Control
LNA Majsat
H3K9me3
rH2AX
DAPI
B
C
D
E
B
C
D
E
Fluorescent intensity(A.U.)
1500
1000
500
0
DAPI
H3K9Me3
F
LNA Control
LNA MajSat
H3K27Me3
G
H3K27Me3
2.0
1.5
1.0
0.5
0.0
*
LNA control
LNA MajSat
H
LNA Control
LNA MajSat
H3K4Me3
I
H3K4Me3
n.s.
4
3
2
1
0
LNA control
LNA Majsat

Fig. S19.

***Major satRNA*s control heterochromatin retention in quiescent NPCs.** (**A-E**) Changes in H3K9me3 and γH2AX after LNA-mediated knock-down of *major satRNAs*. Signal intensities of insets from (B-E) were line scanned and presented below. Note the significant reduction of H3K9me3 signals around the DAPI signal-enriched chromocenter area compared with controls. (**F-G**) LNA-mediated knock-down of *major satRNAs* reduces nuclear H3K27me3 levels. $*P < 0.05$ (unpaired *t*-test, depicted are individual nuclei with mean +/- SD from n = 3 experiments). (**H-I**) LNA-mediated knock-down of *major satRNAs* does not affect nuclear H3K4me3 levels. n.s. not significant (Mann-Whitney test, depicted are individual nuclei with mean +/- SD from n = 3 experiments). Scale bars in A, F, H, 5 μm.

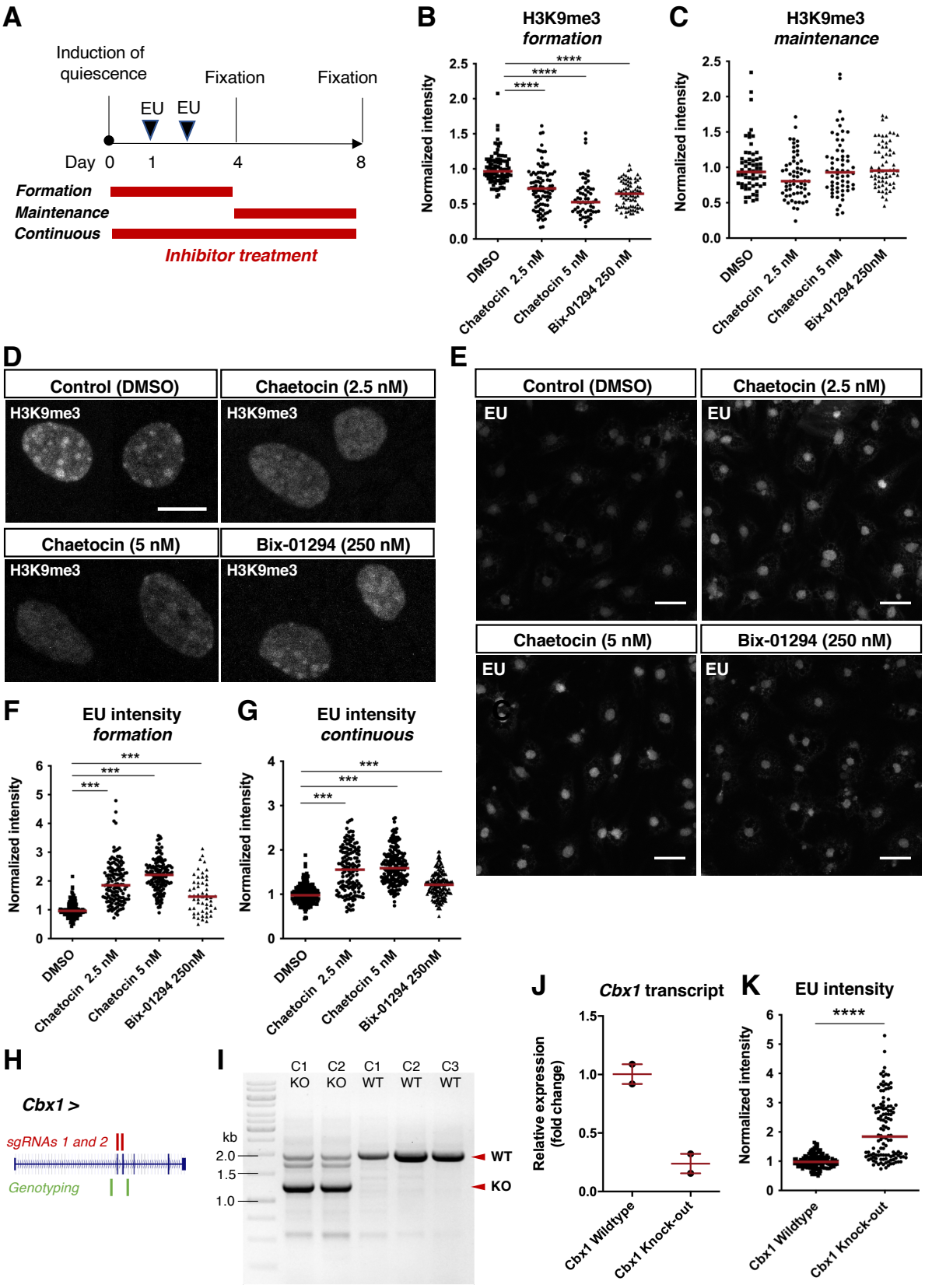
A
Induction of quiescence
Fixation
Fixation
EU EU
Day 0 1 4 8
Formation
Maintenance
Continuous
Inhibitor treatment
B
H3K9me3 formation
Normalized intensity
DMSO
Chaetocin 2.5 nM
Chaetocin 5 nM
Bix-01294 250 nM
C
H3K9me3 maintenance
Normalized intensity
DMSO
Chaetocin 2.5 nM
Chaetocin 5 nM
Bix-01294 250nM
D
Control (DMSO)
Chaetocin (2.5 nM)
Chaetocin (5 nM)
Bix-01294 (250 nM)
H3K9me3
E
Control (DMSO)
Chaetocin (2.5 nM)
Chaetocin (5 nM)
Bix-01294 (250 nM)
EU
F
EU intensity formation
Normalized intensity
DMSO
Chaetocin 2.5 nM
Chaetocin 5 nM
Bix-01294 250nM
G
EU intensity continuous
Normalized intensity
DMSO
Chaetocin 2.5 nM
Chaetocin 5 nM
Bix-01294 250nM
H
Cbx1 >
sgRNAs 1 and 2
Genotyping
I
C1 KO
C2 KO
C1 WT
C2 WT
C3 WT
kb
2.0
1.5
1.0
WT
KO
J
Cbx1 transcript
Relative expression (fold change)
Cbx1 Wildtype
Cbx1 Knock-out
K
EU intensity
Normalized intensity
Cbx1 Wildtype
Cbx1 Knock-out

Fig. S20.

Roles of heterochromatin in LL-RNA regulation in quiescent NPCs. (**A**) Experimental scheme for treatment of quiNPCs with Suv39h1/2 inhibitors. (**B**) Chaetocin and BIX-01294 significantly reduced heterochromatin formation (H3K9me3 levels) during the induction of quiescence in NPCs. (**C**) Chaetocin and BIX-01294 treatment starting at 4 days after induction of quiescence did not significantly reduce heterochromatin maintenance in NPCs. (**D**) Representative images of H3K9me3 immunocytochemistry. Scale bar, 10 µm. (**E**) Representative images of EU staining at day 8. Scale bar, 25 µm. (**F-G**) Suv39h1/2 inhibitors significantly increased nuclear EU levels when applied selectively during EU labelling (F) or continuously for 8 days during NPC quiescence (G). Graphs in B,C,F,G depict intensities for individual nuclei with group medians from n = 3 independent experiments. ***$P < 0.001$ from Wilcoxon-Mann-Whitney test. (**H**) Strategy for CRISPR-based knock-out of *Cbx1*. Cells were transfected with 2 sgRNAs targeting the first two coding exons of *Cbx1* and individual NPC clones were expanded as NPC lines. (**I**) Genotyping PCR identified 2 NPC clonal lines with expected deletions of the first 2 Cbx1 coding exons (C1 KO and C2 KO), whereas clonal control NPC lines showed wildtype (WT) Cbx1 bands (C1-C3 WT). Arrows indicate expected sizes for WT and knock-out (KO) fragments. KO and WT fragments were confirmed by Sanger sequencing. (**J**) Silencing of Cbx1 transcript in both Cbx1 knock down NPC lines compared to control NPC lines. Depicted is the relative expression as determined by qRT-PCR. (**K**) Increased nuclear EU intensity at 1 week after EU labelling in quiescent Cbx1 knock-down NPCs lines compared to control NPC lines. Depicted are EU intensities of individual nuclei with group medians (n = 2 NPC lines). ****$P < 0.001$ from Wilcoxon-Mann-Whitney test.

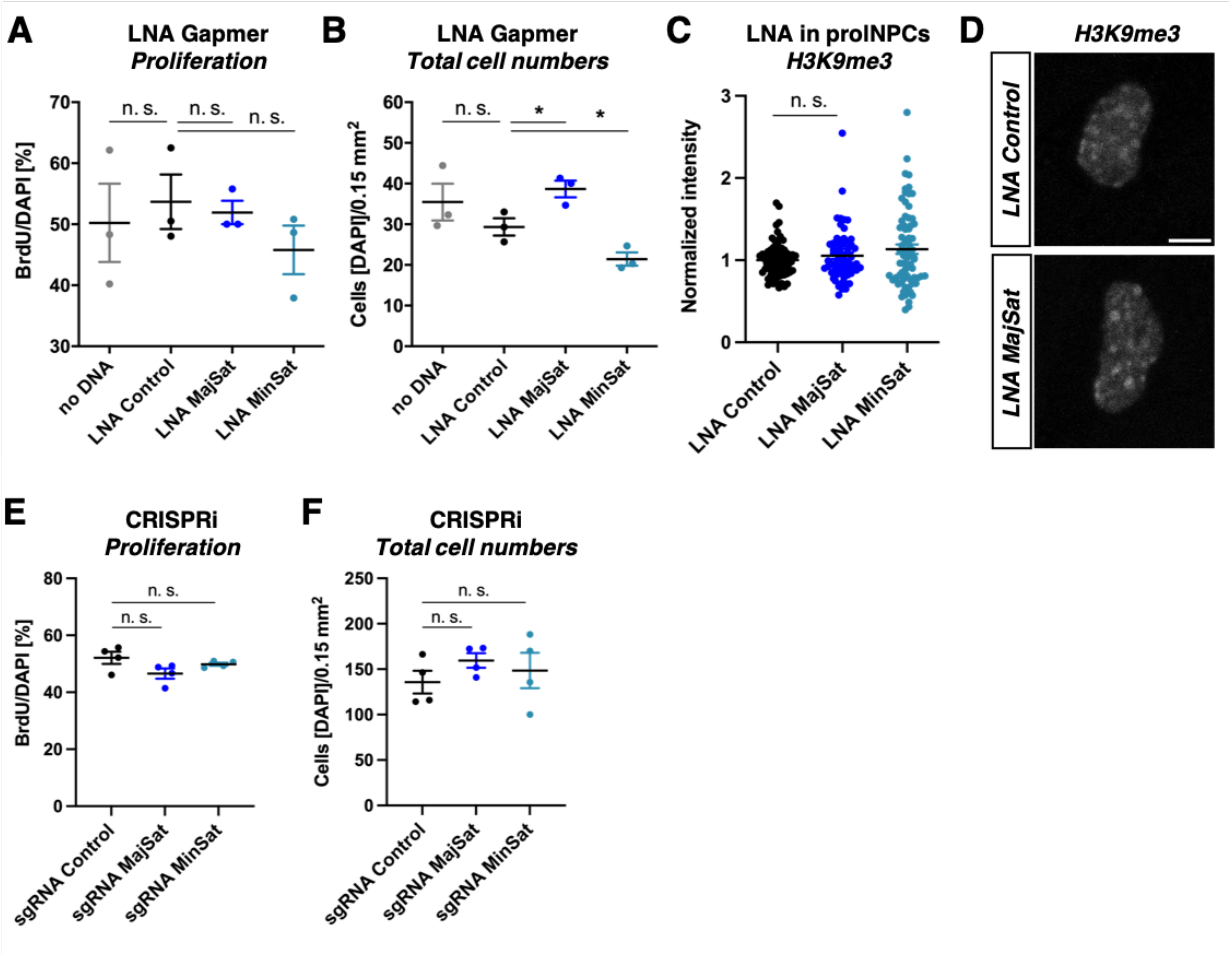

Fig. S21.

Knock-down of *satRNAs* in mitotic NPCs does not affect their proliferation. (**A-D**) LNA-mediated knock-down of *satRNAs* did not affect proliferation nor nuclear H3K9me3 levels in proliferating NPCs. Transfection of the Control LNA GapmeR does not impair NPC proliferation compared to control transfections without LNA GapmeR. NPCs were analyzed 3 days after transfection with LNA GapmeRs. Scale bar in D, 5 µm. (**E-F**) CRISPRi-based transcriptional inhibition of *major* or *minor satRNAs* does not affect proliferative capacity or cell death in proliferating NPCs. NPCs were analyzed 5 days after transfection of sgRNAs and dCas9-KRAB expression vectors. Depicted are individual data points with means +/- SEM. All *P*-values from unpaired *t*-test (*$P < 0.05$, n. s. not significant; n = 3-4 experiments).

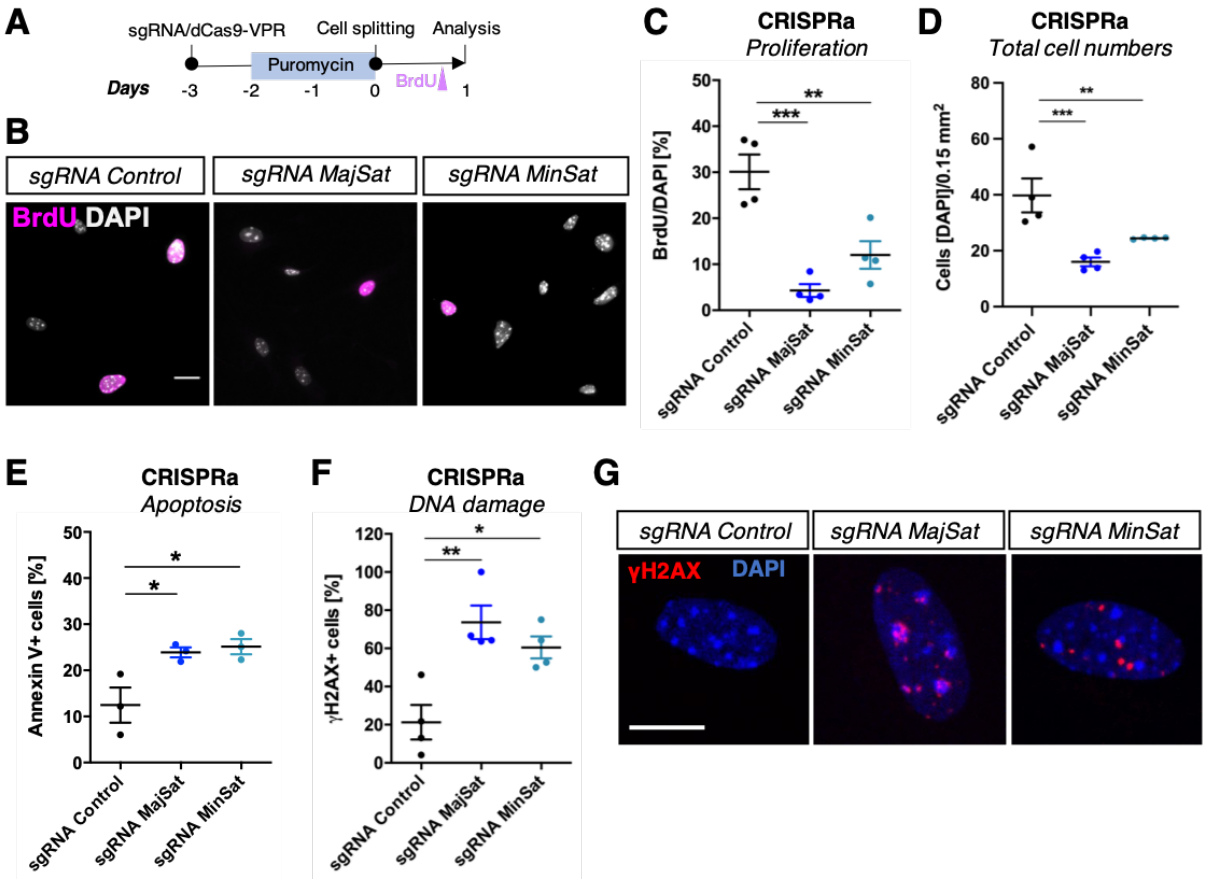

Fig. S22.

Overexpression of *satRNAs* is detrimental for NPCs. (**A**) Experimental scheme. NPCs were transfected with sgRNAs and dCas9-VPR constructs (CRISPRa) and transfected cells were selected using puromycin. NPCs were analyzed 4 days after transfection. (**B**) Representative image of BrdU labeling. Scale bar, 20 µm. (**C-D**) Overexpression of *major* and *minor satRNAs* strongly reduced numbers of proliferating cells. (**E**) Increase in apoptotic cells (Annexin V+) after overexpression of *major* and *minor satRNA*s. (**F**) *SatRNA* overexpression triggered DNA damage (elevated γH2AX) in quiNPCs. Scale bar, 10 µm. Depicted are individual data points with means +/- SEM. All *P*-values are from unpaired *t*-tests (***$P < 0.005$, **$P < 0.01$, *$P < 0.05$; n = 3-4 experiments).

Table S1.

Oligonucleotide name	Used for	Sequence (5'-3')
Gapdh_fw	qRT-PCR	TGAACGGGAAGCTCACTGG
Gapdh_rev	qRT-PCR	TCCACCACCCTGTTGCTGTA
MajSat_fw	qRT-PCR	TGGAATATGGCGAGAAAACTG
MajSat_rev	qRT-PCR	AGGTCCTTCAGTGGGCATTT
MinSat_fw	qRT-PCR	GAACATATTAGATGAGTGAGTTAC
MinSat_rev	qRT-PCR	GTTCTACAAATCCCGTTTCCAAC
SINEB1_fw	qRT-PCR	GTGGCGCACGCCTTTAATC
SINEB1_rev	qRT-PCR	GACAGGGTTTCTCTGTGTAG
28S rRNA_fw	qRT-PCR	TCCTTATCCCGAAGTTACGG
28S rRNA_rev	qRT-PCR	GGGGAGAGGGTGTAAATCTC
18S rRNA_fw	qRT-PCR	ACATCCAAGGAAGGCAGCAG
18S rRNA_rev	qRT-PCR	CATTCCAATTACAGGGCCTC
Actb_fw	qRT-PCR	GCCAACCGTGAAAAGATGAC
Actb_rev	qRT-PCR	CATCACAATGCCTGTGGTAC
L1_ORF1_fw	qRT-PCR	GAACCAAGACCACTCACCATCA
L1_ORF1_rev	qRT-PCR	CCCTGGACTGGGCGAAGT
sgRNA_MajSat_1	CRISPRa/CRISPRi	GAAATGAGAAATGCACACTGT
sgRNA_MajSat_2	CRISPRa/CRISPRi	GAAATGCACACTGTAGGAGC
sgRNA_MinSat_1	CRISPRa/CRISPRi	GAAAAACACATTCGTTGGAAA
sgRNA_Control	CRISPRa/CRISPRi	GACGTGGAGCTGGGGGAAG
sgRNA_Cbx1_1	Cbx1 knock-out	GAAAGCTGGCGGGTACTATG
sgRNA_Cbx1_2	Cbx1 knock-out	GATTCTGATTCTGAAGATAA
Cbx1_fw	Genotyping	TGACTGTGTTCGAGAATAGCG
Cbx1_rev	Genotyping	CACTGTATAAGAGCAAGCCCCA
Control_Gapmer	LNA Gapmer Control	AACACGTCTATACGC
MajSat_Gapmer_1	LNA Gapmer knock-down	ACATCCACTTGACGACTTG
MajSat_Gapmer_2	LNA Gapmer knock-down	TATTTCACGTCCTAAAGTG
MinSat_Gapmer_1	LNA Gapmer knock-down	CGTTGGAAATGGATTA
MinSat_Gapmer_2	LNA Gapmer knock-down	AACTCACTCATCTAAT

List of oligonucleotide sequences.

Data S1. (separate file)

Lists of long-retained transcripts in quiNPCs and hippocampus tissue as identified by EU-RNA-Sequencing.